Infectious Disease Modelling 8 (2023) 717–741

Contents lists available at ScienceDirect

Infectious Disease Modelling

journal homepage: www.keaipublishing.com/idm

Vaccine breakthrough and rebound infections modeling: Analysis for the United States and the ten U.S. HHS regions

Olusegun Michael Otunuga*, Alexandra Yu

Department of Mathematics, Augusta University, 1120 15th Str, GE 2018, Augusta, GA, 30912, USA

ARTICLE INFO

Article history:
Received 28 February 2023
Received in revised form 19 May 2023
Accepted 29 May 2023
Available online 2 June 2023
Handling Editor: Dr He Daihai

Keywords:
Multi-strain
Delta
Omicron
Lineages
Vaccine breakthrough
Rebound infection

ABSTRACT

A vaccine breakthrough infection and a rebound infection cases of COVID-19 are studied and analyzed for the ten U.S. Department of Health and Human Services (HHS) regions and the United States as a nation in this work. An innovative multi-strain susceptible-vaccinated-exposed-asymptomatic-symptomatic-recovered (*SVEAIR*) epidemic model is developed for this purpose for a population assumed to be susceptible to n-different variants of the disease, and those who are vaccinated and recovered from a specific strain $k(k \leq n)$ of the disease are immune to present strain and its predecessors $j = 1, 2, \ldots, k$, but can still be infected by newer emerging strains $j = k + 1, k + 2, \ldots, n$. The model is used to estimate epidemiological parameters, namely, the latent and infectious periods, the transmission rates, vaccination rates, recovery rates for each of the Delta B.1.617.2, Omicron B.1.1.529, and lineages BA.2, BA.2.12.1, BA.4, BA.5, BA.1.1, BA.4.6, and BA.5.2.6 for the United States and for each of the ten HHS regions. The transmission rate is estimated for both the asymptomatic and symptomatic cases. The effect of vaccines on each strain is analyzed. Condition that guarantees existence of an endemic with certain number of strains is derived and used to describe the endemic state of the population.

1. Introduction

Currently, the Omicron variant B.1.1.529 of COVID-19 and its lineages are widely monitored in the United States and around the world. The variant was first detected in specimens collected on November 11, 2021 in Botswana and on November 14, 2021 in South Africa and was first reported by South Africa to the World Health Organization (WHO) on November 24, 2021, with the first confirmed B.1.1.529 infection from a specimen collected on November 9, 2021. European Centre for Disease Prevention and Control (ECDC) first classified the variant as a Variant of Interest (VOI) on November 25, 2021, and later upgraded this to Variant of Concern (VOC) the following day. According to the Center for Disease Control and Prevention (CDC), a VOC is a variant with evidence of increase transmissibility, and having more severe disease with significant reduction in neutralization by antibodies generated during previous infection or vaccination, and reduced effectiveness of treatments or vaccines, or diagnostic detection failures. The first case of this variant was reported in the United States on December 1, 2021. Before the existence of the Omicron B.1.1.529 is the Delta B.1.617.2 variant which was first reported in the United States earlier in January 2020. It was the main circulating variant in the United States as of early December 2021. The infectivity of the Delta variant steadily decreased and was swiftly replaced by the Omicron variant in late November 2021. The Omicron variant becomes the main circulating variant in the United States as of early January 2022, and dominated other VOC by February 2022. Since then, the variant's high transmission pattern has facilitated the occurrence of additional mutations, leading to the emergence of several sublineages including BA.1, BA.2, BA.3, BA.4, BA.5 (as of April 12, 2022 (PAHO/WHO, 2022b)), BA.2.12.1, BA.1.1, B.1.617.2, BQ.1.1, BQ.1, XBB, BF.7, BN.1, BA.5.2.6, BF.11, BA.2.75.2, et.c. as of December 25, 2022. It was discovered that the

* Corresponding author.
E-mail addresses: ootunuga@augusta.edu (O.M. Otunuga), aleyu@augusta.edu (A. Yu).
Peer review under responsibility of KeAi Communications Co., Ltd.

Omicron variant is more likely to mutate in low vaccination rates and high transmission rates (Araf et al., 2022). While BA.2 is predominant in most of the regions at global level around April 12, 2022, the sublineages BA.1 and BA.1.1 are still predominant in the Americas (PAHO/WHO, 2022b). Some of these sublineages have been in circulation before they are reported. The BA.4 and BA.5 were first reported in South Africa on April 04, 2022 and have been circulating since January 2022. The high circulation of BA.1 and BA.2 has facilitated the occurrence of recombination between these two sublineages (PAHO/WHO, 2022b). The high transmission pattern and emergence of new lineages and sublineages of the Omicron variant make estimating epidemiological parameters for the variant and lineages an urgent task for epidemiologists and researchers around the globe.

The variant has continued to grow in number of infections and number of variants, with approximately 100,622,056 cases and 1,088,481 deaths in the United States as of January 2, 2022 as reported by CDC. A total of 657,977,736 cases and 6,681,433 deaths across the world was reported by WHO as of January 7, 2023. During epidemiological week (EW) 50 (December 11, 2022—December 17, 2022), the United States reported a 4.1% increase in weekly hospitalizations and 7.5% increase in ICU admissions for the fifth consecutive week to the WHO (PAHO/WHO, 2022a). According to CDC, the virus' high rate of infection made COVID-19 the third leading cause of death in the United States in 2020.

As changes in the genetic code occur during replication of the genome, viruses like SARS-CoV-2 evolve continuously due to genetic mutations or viral recombination. CDC uses genomic surveillance to identify and track the variants of SARS-CoV-2. The proportion of variants are calculated nationally by HHS regions and jurisdiction. The HHS and their partners are working to execute protective response to the COVID-19 pandemic in terms of health and safety of the American people. The purpose of this study is to determine how threatening COVID-19, specifically the Omicron variant and its lineages are in terms of rate of infection and to determine whether or not any lineage of the variant is predicted to cause an endemic. We analyze which of the sublineages is associated with greater or lesser severity of disease. This is done with the help of the data provided by HHS and CDC. The data helps in studying whether the spread of new variant may be caused by higher transmission rates in certain HHS regions. The estimates of the disease's infectivity, severity, and its impact are crucial for informing rapid policy responses to this potential threat. Few studies have been done to understand the spreading patterns and risks of the virus' pandemic. Mathematical modeling helps in decision-making processes, as well as confirming the effectiveness of public health measures (Rui et al., 2022). Several works have been done (Davies et al., 2021; He et al., 2020; Liu & Rocklöv, 2022; Nishiura et al., 2022; Ogata & Tanaka, 2023; Otunuga, 2021, 2022; Tartof et al., 2022, p. P1663; Ueda et al., 2022; Wang, Zhang, et al., 2022) to study the variants and sublineages of COVID-19 and understand how dangerous each are in terms of infectivity. Mathematical models like the SEIR model (Arruda et al., 2021; Bentaleb et al., 2020; Khyar & Allali, 2020), SIR model (Fudolig & Howard, 2017; Massard et al., 2022; Meehan et al., 2018) and its extensions (Hattaf et al., 2021; Nisar et al., 2021) have been developed to analyze the COVID-19 cases. Some of these existing models did not capture the vaccinated groups, and are usually designed for a scenario where the population is infected by a single variant of the disease. Most of these models usually assume that individuals are protected from a disease once vaccinated, and those who recovered from such disease cannot be re-infected. A Susceptible (Unvaccinated)-Vaccinated-Exposed-Asymptomatic -Symptomatic - Recovered (SVEAIR) epidemic model that assumes vaccine breakthrough and rebound infections is designed in this work to represent the spread of the disease and its variants and lineages. The model assumes a particular population is susceptible to n variants of a disease, with the population divided into disjoint compartments comprising of susceptible (S) individuals that are not vaccinated, population with individuals (V_k) vaccinated against specific strain (say strain k) of the virus, population (E_k) containing individuals exposed to strain k of the virus, population (A_k) of asymptomatic strain-k infected individuals, population (I_k) of symptomatic strain k-infected individuals and population (R_k) of those who recovered from strain-k. Here, we assume that the order of existence of newer strains follow $k = 1, 2, \cdots, n$, with $k = j$ representing the j-th emerging strain. Those who are vaccinated and recovered from a specific strain of the disease are assumed to be immune to present strain and its predecessors, but can still be infected by newer emerging strains. The model is an extension of the work of Otunuga (Otunuga, 2022) who analyzed a vaccine breakthrough case for a population infected by n variants, and extended the model to include a rebound case for two variants. Since only weekly cases of infections are available, the parameters in the model are estimated for each of the ten HHS regions by minimizing the sum of square errors in the weekly infection cases using the Nelder-Mead simplex algorithm (Lagarias et al., 1998).

The paper is organized as follows: In Section 2, the model used in describing the spread of variants and its lineages is formulated and analyzed. Epidemiological metrics, including the reproduction number for each variants/lineages is calculated using the Next Generation Matrix method (Driessche & Watmough, 2002). The model is applied to analyze the weekly variant proportions (Centers for Disease Control and Prevention (CDC), 2022b) and infection cases (Centers for Disease Control and Prevention (CDC), 2022a) for the United States and the ten HHS U.S. regions in Section 3. The epidemiological parameters and reproduction numbers for each strains and each of the ten HHS regions are estimated and used in describing the endemic state of the variants. Sensitivity analysis is carried out to know which epidemiological parameters in the model has the highest impact on the disease transmission and prevalence. The summary of the work done is discussed in Section 4.

2. Modeling vaccine breakthrough and rebound infection: general model

In this section, we assume a vaccine breakthrough (a situation where someone who is vaccinated with either a primary series or a primary series plus a booster dose gets infected with the virus that causes COVID-19) and rebound infection cases. According to CDC, people who are vaccinated and recovered from COVID-19 can still be infected by the virus. Consider a

scenario where those who recovered from a particular strain (or (sub)lineage) k and those who get vaccinated against strain k are immune to the strain and its predecessors but can still be infected by emerging strain $j, j > k$ ($k = 1, 2, \ldots, n$, with n total number of strains in the population at the given time). We assume susceptible non vaccinated individuals get infected with the virus when in contact with asymptomatic and symptomatic infectious individuals A_k and I_k, respectively, at a rate β which is directly proportional to A_k and I_k and described by $\beta = \sum_{k=1}^{n} (\gamma_k A_k + \beta_k I_k)$, where γ_k and β_k are the transmission rates of the asymptomatic and symptomatic strain-k infectious individuals, respectively. Individuals (V_k) vaccinated against strain k are immune to the strain and its predecessors, and can only be infected by asymptomatic and symptomatic infectious individuals A_j and I_j, $j > k$ with emerging strains/lineages of the virus, respectively, at a rate $\sum_{j=k+1}^{n} \left(\gamma_j A_j + \beta_j I_j\right)$. The force of strain-$k$ infection on the susceptible population is equal to $\gamma_k A_k + \beta_k I_k$. Since individuals in group V_k are vaccinated against strain k and its predecessors, then the force of infection $\gamma_k A_k + \beta_k I_k$ only acts on the group $V_1, \ldots, V_{k-1}$. Likewise, since those who recovered from strain k can still be infected by emerging strain, then the force of infection $\gamma_k A_k + \beta_k I_k$ acts on the group $R_1, \ldots, R_{k-1}$. Asymptomatic and symptomatic infectious individuals with strain k are assumed to recover at constant rates r_k and θ_k, respectively. Individuals exposed to strain k become infectious at a rate λ_k, where only a fraction p_k of strain-k exposed individuals progress to the asymptomatic infectious compartment A_k. The states and parameters in the model are described in Tables 1 and 2, respectively.

The model describing the spread of the virus in the population is given by

$$
\begin{aligned}
dS &= \left((1-q)\mu - S\sum_{j=1}^{n}\left(\beta_j I_j + \gamma_j A_j\right) - \mu S \right) dt, \quad S(t_0) = S_0,\\
dV_k &= \left(q_k\mu - V_k \sum_{j=k+1}^{n} \left(\beta_j I_j + \gamma_j A_j\right) - \mu V_k \right) dt, \quad V_k(t_0) = V_{k0}, \quad k = 1, 2, \ldots, n-1,\\
dV_n &= (q_n\mu - \mu V_n)dt, \quad V_n(t_0) = V_{n0},\\
dE_1 &= (S(\beta_1 I_1 + \gamma_1 A_1) - (\mu + \lambda_1)E_1)\, dt, \quad E_1(t_0) = E_{10},\\
dE_k &= \left(S(\beta_k I_k + \gamma_k A_k) + \sum_{j=1}^{k-1} V_j(\beta_k I_k + \gamma_k A_k) + \sum_{j=1}^{k-1} R_j(\beta_k I_k + \gamma_k A_k) - (\mu + \lambda_k)E_k \right) dt, \quad E_k(t_0) = E_{k0}, \quad k = 2, 3, \ldots, n,\\
dA_k &= (p_k\lambda_k E_k - (\mu + r_k)A_k)\, dt, \quad k = 1, 2, \ldots, n \quad A_k(t_0) = A_{k0}, \quad k = 1, 2, \ldots, n,\\
dI_k &= ((1-p_k)\lambda_k E_k - (\mu + \theta_k)I_k)\, dt, \quad I_k(t_0) = I_{k0}, \quad k = 1, 2, \ldots, n,\\
dR_k &= \left(\theta_k I_k + r_k A_k - R_k \sum_{j=k+1}^{n} \left(\beta_j I_j + \gamma_j A_j\right) - \mu R_k \right) dt, \quad R_k(t_0) = R_{k0}, \quad k = 1, 2, \ldots, n-1,\\
dR_n &= (\theta_n I_n + r_n A_n - \mu R_n)\, dt, R_n(t_0) = R_{n0}.
\end{aligned}
\tag{2.1}
$$

Table 1
Description of variables for the epidemic model.

Variable	Description
S	Population of susceptible individuals
V_k	Population of vaccinated individuals immune to strain k of the infection
E_k	Population of individuals exposed to strain k of the infection
A_k	Population of asymptomatic individuals infected with strain k of the infection
I_k	Population of symptomatic individuals infected with strain k of the infection
R_k	Population of individuals who recovered from the k-th strain

Table 2
Description of parameters for the epidemic model.

Parameter	Description
β_k	Transmission rate of symptomatic infected individuals
γ_k	Transmission rate of asymptomatic infected individuals
μ	Birth/death rate
p_k	Fraction of strain k infection cases that are asymptomatic
q_k	Fraction of population vaccinated against strain k of infection
λ_k	Transition rate of individuals with strain k of infection from exposed to infectious class
r_k	Asymptomatic recovery rate of those with strain k of infection
θ_k	Symptomatic recovery rate of those with strain k of infection
q	$\sum_{j=1}^{n} q_j$

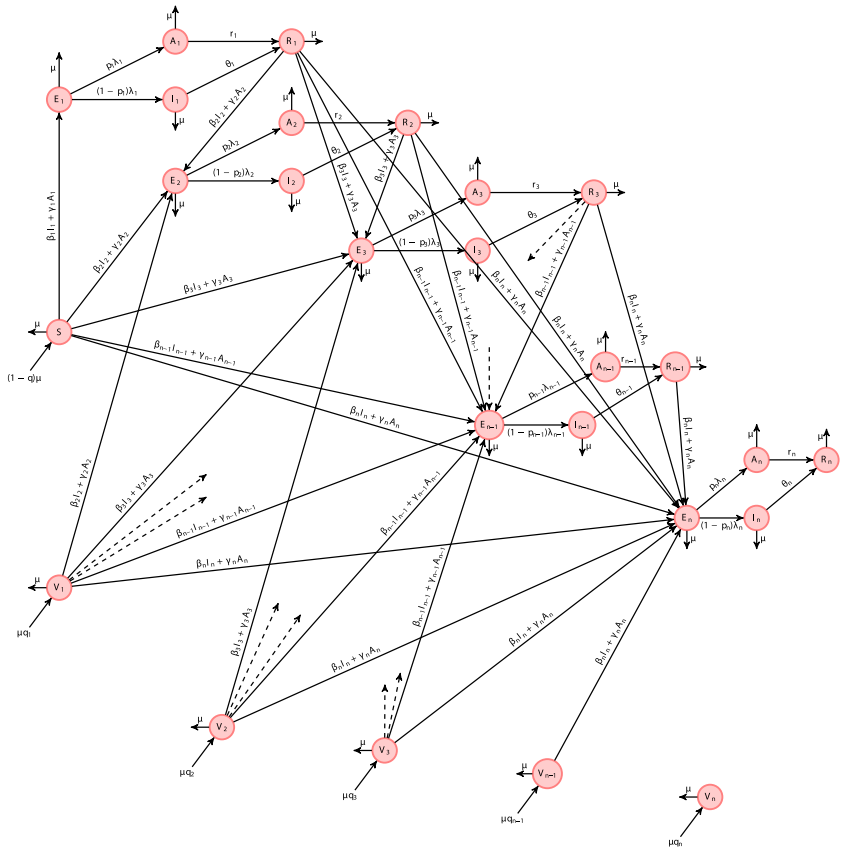

Fig. 1. Schematic diagram for the epidemic model (2.1). The circle compartments represent group of individuals.

The model described here is an extension of the work described in Otunuga (Otunuga, 2022). A schematic diagram of the model is given in Fig. 1.

We discuss the solution of (2.1) in the feasible region

$$\mathcal{T} = \left\{ (S, \{V_k\}_{k=1}^n, \{E_k\}_{k=1}^n, \{A_k\}_{k=1}^n, \{I_k\}_{k=1}^n, \{R_k\}_{k=1}^n) \in \mathbb{R}_+^{5n+1} \mid 0 \le S + \sum_{k=1}^{n} (V_k + E_k + A_k + I_k + R_k) \le 1 \right\}. \tag{2.2}$$

Define

$$\begin{aligned} a_j &= \mu + r_j, \\ e_j &= \mu + \lambda_j, \\ w_j &= \mu + \theta_j, \\ c_j &= (1-p_j)a_j\beta_j + p_j w_j \gamma_j, \\ \bar{c}_j &= (1-p_j)a_j\theta_j + p_j w_j r_j, \quad j = 1, 2, \ldots, n. \end{aligned} \tag{2.3}$$

The reproduction number for each variants/strains is obtained in the following section.

2.1. Reproduction number

The disease-free equilibrium of system (2.1) is

$$\mathcal{E}_0 = \{S^0 = (1-q)\mu, V_k^0 = q_k\mu, E_k^0 = 0, A_k^0 = 0, I_k^0 = 0, R_k^0 = 0, \ k = 1, 2, \ldots, n\}. \tag{2.4}$$

For each strain k, $k = 1, 2, \ldots, n$, we calculate two key epidemiological metrics used in estimating average number of secondary infections caused by an infected individual. We define the effective reproduction number for strain-k, denoted $\mathcal{R}_k$, as the expected number of new infections produced by a strain-k infectious individual in a population where some individuals may no longer be susceptible to some strains (due to some interventions, including vaccination in this case) completely

unvaccinated susceptible population where everyone is assumed to be susceptible, we denote the basic reproduction number by $\mathcal{R}_{c,k}$. These two metrics will be used to track pandemic progress for each of the strains analyzed for the ten HHS regions and the nation in Section 3. Define

$$Q_k = \sum_{j=1}^{k} q_{j-1}, \tag{2.5}$$

where $q_0 = 0$. It was shown in the work of Otunuga (Otunuga, 2022) using the Next Generation Matrix approach (Driessche & Watmough, 2002) that the strain-k reproduction numbers $\mathcal{R}_k$ and $\mathcal{R}_{c,k}$ are obtained as

$$\begin{aligned} \mathcal{R}_k &= (1-q+Q_k)\frac{c_k\lambda_k}{a_k e_k w_k}, \quad k = 1, 2, \ldots, n, \\ \mathcal{R}_{c,k} &= \frac{\mathcal{R}_k}{(1-q+Q_k)}, \quad k = 1, 2, \ldots, n. \end{aligned} \tag{2.6}$$

The population's effective and basic reproduction numbers, denoted $\mathcal{R}_0$ and $\mathcal{R}_{c,0}$, respectively, are obtained as

$$\begin{aligned} \mathcal{R}_0 &= \max_{1\le j\le n}\{\mathcal{R}_j\}, \\ \mathcal{R}_{c,0} &= \max_{1\le j\le n}\{\mathcal{R}_{c,j}\}. \end{aligned} \tag{2.7}$$

2.2. The long term behavior of system (2.1)

We discuss conditions under which there is an endemic with a particular strain in the population on the long run. As discussed in Otunuga (Otunuga, 2022), we give some definitions of terminologies used in identifying the various equilibrium points of the system.

Definition 1. The number τ_k represents the k-th strain in the population, with $k = 0, 1, 2, \ldots, n$ and $k = 0$ representing no strain.

Definition 2. Let $P = \{1, 2, \ldots, n\}$ denotes set of indices representing order of existence of new strain in the population, with 2^P denoting the power set of P. The set $\mathcal{S}_r = \{\tau_1, \tau_2, \ldots, \tau_r\}$ denotes a subset of 2^P with r number of strains $\tau_1, \tau_2, \ldots, \tau_r$ in the population, for $r = 1, 2, \ldots, n$, and $\mathcal{S}_0$ representing the set with no strain in the population.

Definition 3. We denote the disease-free equilibrium point by $\mathcal{E}_{\mathcal{S}_0}$ and described as the equilibrium point for the case where there is no disease in the population on the long run (case where $r = 0$).

Definition 4. We define the equilibrium point $\mathcal{E}_{\mathcal{S}_r}$ as the equilibrium point with r strains $\tau_1, \tau_2, \ldots, \tau_r$ in the population on the long run.

The existence of the equilibrium points $\mathcal{E}_{\mathcal{S}_1}$ and $\mathcal{E}_{\mathcal{S}_2}$, together with their respective global stability conditions, are given in the work of Otunuga (Otunuga, 2022). We state theorems without proof of these existence in Theorems 2.1 and 2.3. In this work, we extend the work of Otunuga (Otunuga, 2022) by proving the existence of the equilibrium point $\mathcal{E}_{\mathcal{S}_r}$, for the case where $r = 3, 4, \ldots, n$, in Theorem 2.4. In Theorem 2.1, we show that strain m alone persists on the long run if the expected number of secondary infections produced by strain m infected individual is greater than one and that produced by other strains is less than one.

Theorem 2.1. *The equilibrium point with only one strain infectivity (referred to as strain τ_1 equilibrium point and denoted $\mathcal{E}_{\mathcal{S}_1}$) for the epidemic model (2.1) is obtained as*

$$\mathcal{E}_{\mathcal{S}_1} = \{S^*, V_1^*, \ldots, V_n^*, E_1^*, \ldots, E_n^*, A_1^*, \ldots, A_n^*, I_1^*, \ldots, I_n^*, R_1^*, \ldots, R_n^*\}, \tag{2.8}$$

where

$$E^*_{\tau_1} = \frac{\mu(1-q+Q_{\tau_1})}{e_{\tau_1}} \frac{(\mathcal{R}_{\tau_1}-1)}{\mathcal{R}_{\tau_1}}$$
$$S^* = \frac{(1-q)}{\mathcal{R}_{\tau_1}}$$
$$V^*_k = \begin{cases} \frac{q_k}{\mathcal{R}_{\tau_1}}, & \text{if } k < \tau_1, \\ q_k, & \text{if } k \geq \tau_1, \end{cases}$$
$$A^*_{\tau_1} = \frac{p_{\tau_1}\lambda_{\tau_1}}{a_{\tau_1}} E^*_{\tau_1},$$
$$I^*_{\tau_1} = \frac{(1-p_{\tau_1})\lambda_{\tau_1}}{w_{\tau_1}} E^*_{\tau_1},$$
$$R^*_{\tau_1} = \frac{\bar{c}_{\tau_1}\lambda_{\tau_1}}{\mu a_{\tau_1} w_{\tau_1}} E^*_{\tau_1}, \tag{2.9}$$

and $E^*_k = A^*_k = I^*_k = R^*_k = 0$ for $1 \leq k \neq \tau_1 \leq n$, provided $\mathcal{R}_{\tau_1} > 1$.

Proof. The proof follows from Theorem 2 of Otunuga (Otunuga, 2022). ■

In the next theorem, we show that this equilibrium point is globally stable in the feasible region $\mathcal{T}$ provided $\mathcal{R}_k \leq 1$ for all $1 \leq k \neq \tau_1 \leq n$ and $\mathcal{R}_{\tau_1} > 1$.

Theorem 2.2. *The strain-τ_1 equilibrium $\mathcal{E}_{\mathcal{S}_1}$ for the epidemic model (2.1) is globally stable in the feasible region $\mathcal{T}$* if $\mathcal{R}_k \leq 1$ for all $1 \leq k \neq \tau_1 \leq n$ and $\mathcal{R}_{\tau_1} > 1$.

Proof. The proof follows from Theorem 8 of Otunuga (Otunuga, 2022). ■

Define

$$\overline{\mathcal{R}}_{\tau_k} = (1-q+Q_{\tau_k}) \frac{\bar{c}_{\tau_k}\lambda_{\tau_k}}{a_{\tau_k} e_{\tau_k} w_{\tau_k}}, \quad k = 1, 2, \ldots, n. \tag{2.10}$$

Clearly, it follows from (2.3) that

$$\overline{\mathcal{R}}_{\tau_k} < 1 - q + Q_{\tau_k}. \tag{2.11}$$

Theorem 2.3. *The epidemic model (2.1) has an equilibrium point $\mathcal{E}_{\mathcal{S}_2}$ obtained as*

$$\mathcal{E}_{\mathcal{S}_2} = \{S^+, V^+_1, \ldots, V^+_n, E^+_1, \ldots, E^+_n, A^+_1, \ldots, A^+_n, I^+_1, \ldots, I^+_n, R^+_1, \ldots, R^+_n\}, \tag{2.12}$$

where

$$E^+_{\tau_1} = \frac{\mu}{e_{\tau_1}} \frac{\mathcal{R}_{\tau_1} - \mathcal{R}_{\tau_2}}{\frac{\mathcal{R}_{\tau_1}}{1-q+Q_{\tau_1}} - \frac{\mathcal{R}_{\tau_2}}{1-q+Q_{\tau_2}} \left(1 - \frac{\overline{\mathcal{R}}_{\tau_1}}{1-q+Q_{\tau_1}}\right)}$$

,

$$E^+_{\tau_2} = \frac{\mu}{e_{\tau_2}} \left(\frac{1-q+Q_{\tau_2}}{\mathcal{R}_{\tau_2}}\right) \frac{\frac{\mathcal{R}_{\tau_2}}{1-q+Q_{\tau_2}} + (Q_{\tau_2} - Q_{\tau_1}) \frac{\mathcal{R}_{\tau_1}}{1-q+Q_{\tau_1}} \frac{\mathcal{R}_{\tau_2}}{1-q+Q_{\tau_2}} - \frac{\mathcal{R}_{\tau_1}}{1-q+Q_{\tau_1}} + \frac{\mathcal{R}_{\tau_2}}{1-q+Q_{\tau_2}} \frac{\overline{\mathcal{R}}_{\tau_1}}{1-q+Q_{\tau_1}} (\mathcal{R}_{\tau_1} - 1)}{\frac{\mathcal{R}_{\tau_1}}{1-q+Q_{\tau_1}} - \frac{\mathcal{R}_{\tau_2}}{1-q+Q_{\tau_2}} \left(1 - \frac{\overline{\mathcal{R}}_{\tau_1}}{1-q+Q_{\tau_1}}\right)},$$

$$S^+ = \frac{1-q}{\mathcal{R}_{\tau_1}}, V^+_k = \begin{cases} \frac{q_k}{\mathcal{R}_{\tau_1}}, & \text{if } k \leq \tau_1 - 1, \\ \frac{q_k \mu}{\mu + \frac{c_{\tau_2}\lambda_{\tau_2}}{a_{\tau_2} w_{\tau_2}} E^+_{\tau_2}}, & \text{if } \tau_1 \leq k < \tau_2, \\ q_k, & \text{if } k \geq \tau_2, \end{cases}$$

$$A^+_{\tau_k} = \frac{p_{\tau_k}\lambda_{\tau_k}}{a_{\tau_k}} E^+_{\tau_k}, \quad k = 1, 2,$$

$$I^+_{\tau_k} = \frac{(1-p_{\tau_k})\lambda_{\tau_k}}{w_{\tau_k}} E^+_{\tau_k}, \quad k = 1, 2,$$

$$R^+_{\tau_1} = \frac{\bar{c}_{\tau_1}\lambda_{\tau_1}}{a_{\tau_1} w_{\tau_1}} \frac{E^+_{\tau_1}}{\mu + \frac{c_{\tau_2}\lambda_{\tau_2}}{a_{\tau_2} w_{\tau_2}} E^+_{\tau_2}},$$

$$R^+_{\tau_2} = \frac{\bar{c}_{\tau_2}\lambda_{\tau_2}}{\mu a_{\tau_2} w_{\tau_2}} E^+_{\tau_2}, \tag{2.13}$$

$E^+_k = A^+_k = I^+_k = R^+_k = 0$ for $k \neq \tau_1, \tau_2$, in the feasible region $\mathcal{T}$ provided

$$\mathcal{R}_{\tau_1} > \mathcal{R}_{\tau_2} > 1 + \frac{\mathcal{R}_{\tau_1} - 1}{1 + \frac{Q_{\tau_2} - Q_{\tau_1} + \overline{\mathcal{R}}_{\tau_1}}{1 - q + Q_{\tau_1} - \overline{\mathcal{R}}_{\tau_1}}} \mathcal{R}_{\tau_1}, \tag{2.14}$$

is satisfied.

Proof. The proof follows from Theorem 13 of Otunuga (Otunuga, 2022). ■

Remark 2.2.1. Since the function $f(x) = \frac{Q_{\tau_2} - Q_{\tau_1} + x}{1 - q + Q_{\tau_1} - x}$ is an increasing function of x for $0 < x < 1 - q + Q_{\tau_1}$, it follows that $f(\overline{\mathcal{R}}_{\tau_1}) > f(0)$ so that the condition

$$\mathcal{R}_{\tau_1} > \mathcal{R}_{\tau_2} > 1 + \frac{\mathcal{R}_{\tau_1} - 1}{1 + \frac{Q_{\tau_2} - Q_{\tau_1}}{1 - q + Q_{\tau_1}} \mathcal{R}_{\tau_1}} \tag{2.15}$$

also implies (2.14). The equilibrium point $\mathcal{E}_{\mathcal{S}_2}$ is globally stable in the feasible region $\mathcal{T}$ provided that condition (2.14) is satisfied and $\mathcal{R}_k \leq 1$ for all $1 \leq k \neq \tau_1, \tau_2 \leq n$. The proof of this was shown in Otunuga (Otunuga, 2022). In the following theorem, we calculate the epidemiological conditions that guarantee the persistence of r number of strains in the population on the long run, with $r = 3, 4, \ldots, n$. The conditions that guarantee the existence of $r = 1$ strain and $r = 2$ strains are shown in Theorems 2.1 and 2.3, respectively.

Define

$$\begin{aligned} F_{\tau_k} &= \mathcal{R}_{c,\tau_k}\mathcal{R}_{c,\tau_{k+1}}(Q_{\tau_{k+1}} - Q_{\tau_k})\mu, \\ G_{\tau_k} &= \mathcal{R}_{c,\tau_k}\mathcal{R}_{c,\tau_{k+1}} e_{\tau_k} \overline{\mathcal{R}}_{c,\tau_k} \\ H_{\tau_k} &= \mathcal{R}_{c,\tau_k} - \mathcal{R}_{c,\tau_{k+1}}, \end{aligned},$$

for $k = 1, 2, \ldots, r-1$, where $\mathcal{R}_{c,\tau_k}$ is defined in (2.6) and

$$\overline{\mathcal{R}}_{c,\tau_k} = \frac{\overline{\mathcal{R}}_{\tau_k}}{1 - q + Q_{\tau_k}}, \quad k = 1, 2, \ldots, n.$$

Theorem 2.4. *For $r = 3, 4, \ldots, n$, the strain-$\mathcal{S}_r$ equilibrium point*

$$\mathcal{E}_{\mathcal{S}_r} = \{S^-, V^-_1, \ldots, V^-_n, E^-_1, \ldots, E^-_n, A^-_1, \ldots, A^-_n, I^-_1, \ldots, I^-_n, R^-_1, \ldots, R^-_n\}, \tag{2.16}$$

of system *(2.1)* exists in the feasible region $\mathcal{T}$, where

$$S^- = \frac{(1-q)\mu}{\mu + \sum_{j=1}^{r} \left(\frac{c_{\tau_j}\lambda_{\tau_j}}{a_{\tau_j} w_{\tau_j}} E^-_{\tau_j} \right)} = \frac{1-q}{\mathcal{R}_{\tau_1}},$$

$$V^-_k = \begin{cases} \dfrac{q_k \mu}{\mu + \sum_{j=l}^{r} \left(\frac{c_{\tau_j}\lambda_{\tau_j}}{a_{\tau_j} w_{\tau_j}} E^-_{\tau_j} \right)}, & \text{if} \quad \tau_{l-1} \leq k \leq \tau_l - 1, \quad l = 1, 2 \cdots, r, \quad \tau_0 = 1, \\ q_k, \quad \text{if} \quad \tau_r \leq k \leq n, \end{cases}$$

$$E^-_{\tau_1} = \frac{\mu}{e_{\tau_1}} \frac{\mathcal{R}_{\tau_1} - \mathcal{R}_{\tau_2}}{\frac{\mathcal{R}_{\tau_1}}{1 - q + Q_{\tau_1}} - \frac{\mathcal{R}_{\tau_2}}{1 - q + Q_{\tau_2}} \left(1 - \frac{\overline{\mathcal{R}}_{\tau_1}}{1 - q + Q_{\tau_1}} \right)},$$

$$E^-_{\tau_2} = \varphi_{\tau_1} E^-_{\tau_1} + \eta_{\tau_1},$$

$$
\begin{aligned}
E^-_{\tau_k} &= \left(\prod_{j=1}^{k-1}\varphi_{\tau_j}\right)E^-_{\tau_1} + \sum_{m=2}^{k-1}\left(\prod_{j=1}^{k-m}\varphi_{\tau_{k-j}}\right)\eta_{\tau_{m-1}} + \eta_{\tau_{k-1}}, \quad \text{for} \quad k = 3,4,\ldots,r-1,\\
E^-_{\tau_r} &= \frac{G_{\tau_{r-1}}}{e_{\tau_r}\mathcal{R}_{c,\tau_r}H_{\tau_{r-1}}}E^-_{\tau_{r-1}} + \frac{F_{\tau_{r-1}} - \mu H_{\tau_{r-1}}}{e_{\tau_r}\mathcal{R}_{c,\tau_r}H_{\tau_{r-1}}},\\
A^-_{\tau_k} &= \frac{p_{\tau_k}\lambda_{\tau_k}}{a_{\tau_k}}E^-_{\tau_k}, \quad k = 1,2\cdots,r,\\
I^-_{\tau_k} &= \frac{(1-p_{\tau_k})\lambda_{\tau_k}}{w_{\tau_k}}E^-_{\tau_k}, \quad k = 1,2\cdots,r,\\
R^-_{\tau_k} &= \frac{\dfrac{\overline{c}_{\tau_k}\lambda_{\tau_k}}{a_{\tau_k}w_{\tau_k}}E^-_{\tau_k}}{\mu + \sum\limits_{j=k+1}^{r}\left(\dfrac{c_{\tau_j}\lambda_{\tau_j}}{a_{\tau_j}w_{\tau_j}}E^-_{\tau_j}\right)}, \quad k = 1,2\cdots,r-1,\\
R^-_{\tau_r} &= \frac{\overline{c}_{\tau_r}\lambda_{\tau_r}}{\mu a_{\tau_r}w_{\tau_r}}E^-_{\tau_r},
\end{aligned}
\tag{2.17}
$$

and $E^-_k = A^-_k = I^-_k = R^-_k = 0$ for $k \notin \mathcal{E}_{\mathcal{S}_r}$, provided

$$
\begin{aligned}
\mathcal{R}_{\tau_{k-1}} \quad > \quad \mathcal{R}_{\tau_k} &> \frac{(1-q+Q_{\tau_k})(Q_{\tau_{k+1}} - Q_{\tau_{k-1}})\dfrac{\mathcal{R}_{\tau_{k-1}}}{1-q+Q_{\tau_{k-1}}}\dfrac{\mathcal{R}_{\tau_{k+1}}}{1-q+Q_{\tau_{k+1}}}}{(Q_{\tau_{k+1}} - Q_{\tau_k})\dfrac{\mathcal{R}_{\tau_{k+1}}}{1-q+Q_{\tau_{k+1}}} + (Q_{\tau_k} - Q_{\tau_{k-1}})\dfrac{\mathcal{R}_{\tau_{k-1}}}{1-q+Q_{\tau_{k-1}}}}, \quad \text{for} \quad k = 2,3,\ldots,r-1,\\
\mathcal{R}_{\tau_r} \quad > \quad 1 &+ \frac{\mathcal{R}_{\tau_{r-1}} - 1}{1 + (Q_{\tau_r} - Q_{\tau_{r-1}})\dfrac{\mathcal{R}_{\tau_{r-1}}}{1-q+Q_{\tau_{r-1}}}},
\end{aligned}
\tag{2.18}
$$

where

$$
\begin{aligned}
\varphi_{\tau_k} &= \frac{H_{\tau_{k+1}}G_{\tau_k}}{H_{\tau_k}(G_{\tau_{k+1}} + H_{\tau_{k+1}}e_{\tau_{k+1}}\mathcal{R}_{c,\tau_{k+1}})},\\
\eta_{\tau_k} &= \frac{H_{\tau_{k+1}}F_{\tau_k} - H_{\tau_k}F_{\tau_{k+1}}}{H_{\tau_k}(G_{\tau_{k+1}} + H_{\tau_{k+1}}e_{\tau_{k+1}}\mathcal{R}_{c,\tau_{k+1}})}.
\end{aligned}
$$

Proof. Assume condition (2.18) is satisfied. Let $\mathcal{E}_{\mathcal{S}_r}$ in (2.16) be an equilibrium point of (2.1) with strains in $\mathcal{S}_r$ so that $E^-_k = A^-_k = I^-_k = R^-_k = 0$ for $k \notin \mathcal{S}_r$. It follows from (2.1) that

$$
\begin{aligned}
S^- &= \frac{(1-q)\mu}{\mu + \sum\limits_{j=1}^{r}\left(\dfrac{c_{\tau_j}\lambda_{\tau_j}}{a_{\tau_j}w_{\tau_j}}E^-_{\tau_j}\right)} = \frac{1-q}{\mathcal{R}_{\tau_1}},\\
V^-_k &= \begin{cases} \dfrac{q_k\mu}{\mu + \sum\limits_{j=l}^{r}\left(\dfrac{c_{\tau_j}\lambda_{\tau_j}}{a_{\tau_j}w_{\tau_j}}E^-_{\tau_j}\right)}, & \text{if} \quad \tau_{l-1} \le k \le \tau_l - 1, \quad l = 1,2\cdots,r, \quad \tau_0 = 1,\\ q_k, \quad \text{if} \quad \tau_r \le k \le n, \end{cases}\\
A^-_{\tau_k} &= \frac{p_{\tau_k}\lambda_{\tau_k}}{a_{\tau_k}}E^-_{\tau_k}, \quad k = 1,2\cdots,r,\\
I^-_{\tau_k} &= \frac{(1-p_{\tau_k})\lambda_{\tau_k}}{w_{\tau_k}}E^-_{\tau_k}, \quad k = 1,2\cdots,r,\\
R^-_{\tau_k} &= \frac{\dfrac{\overline{c}_{\tau_k}\lambda_{\tau_k}}{a_{\tau_k}w_{\tau_k}}E^-_{\tau_k}}{\mu + \sum\limits_{j=k+1}^{r}\left(\dfrac{c_{\tau_j}\lambda_{\tau_j}}{a_{\tau_j}w_{\tau_j}}E^-_{\tau_j}\right)}, \quad k = 1,2\cdots,r-1,
\end{aligned}
$$

$$R^-_{\tau_r} = \frac{\overline{c}_{\tau_r}\lambda_{\tau_r}}{\mu a_{\tau_r} w_{\tau_r}} E^-_{\tau_r}, \tag{2.19}$$

where $E^-_{\tau_k}, k = 1, 2, \ldots, r$ satisfy the equations

$$\mu + \sum_{j=1}^{r}\left(\frac{c_{\tau_j}\lambda_{\tau_j}}{a_{\tau_j} w_{\tau_j}} E^-_{\tau_j}\right) = \mu \mathcal{R}_{\tau_1}, \tag{2.20}$$

$$\mathcal{R}_{c,\tau_{k-1}}\mathcal{R}_{c,\tau_k}\left((Q_{\tau_k} - Q_{\tau_{k-1}})\mu + e_{\tau_{k-1}}\overline{\mathcal{R}}_{c,\tau_{k-1}} E^-_{\tau_{k-1}}\right) + (\mathcal{R}_{c,\tau_k} - \mathcal{R}_{c,\tau_{k-1}})\left(\mu + \sum_{j=k}^{r}\left(\frac{c_{\tau_j}\lambda_{\tau_j}}{a_{\tau_j} w_{\tau_j}} E^-_{\tau_j}\right)\right) = 0, \tag{2.21}$$

for $k = 2, 3, \ldots, r$, where $\mathcal{R}_{c,\tau_k}$ is defined in (2.6). Substituting $\sum_{j=k}^{r}\left(\frac{c_{\tau_j}\lambda_{\tau_j}}{a_{\tau_j} w_{\tau_j}} E^-_{\tau_j}\right) = \mu(\mathcal{R}_{\tau_1} - 1) - \sum_{j=1}^{k-1}\left(\frac{c_{\tau_j}\lambda_{\tau_j}}{a_{\tau_j} w_{\tau_j}} E^-_{\tau_j}\right)$ from (2.20) into (2.21), we have

$$\mathcal{R}_{c,\tau_{k-1}}\mathcal{R}_{c,\tau_k}\left((Q_{\tau_k} - Q_{\tau_{k-1}})\mu + e_{\tau_{k-1}}\overline{\mathcal{R}}_{c,\tau_{k-1}} E^-_{\tau_{k-1}}\right) + (\mathcal{R}_{c,\tau_k} - \mathcal{R}_{c,\tau_{k-1}})\left(\mu\mathcal{R}_{\tau_1} - \sum_{j=1}^{k-1}\left(\frac{c_{\tau_j}\lambda_{\tau_j}}{a_{\tau_j} w_{\tau_j}} E^-_{\tau_j}\right)\right) = 0 \tag{2.22}$$

for $k = 2, 3, \ldots, r$. For $k = 2$, it follows from (2.22) that

$$E^-_{\tau_1} = \frac{\mu}{e_{\tau_1}} \frac{\mathcal{R}_{\tau_1} - \mathcal{R}_{\tau_2}}{\frac{\mathcal{R}_{\tau_1}}{1-q+Q_{\tau_1}} - \frac{\mathcal{R}_{\tau_2}}{1-q+Q_{\tau_2}}\left(1 - \frac{\overline{\mathcal{R}}_{\tau_1}}{1-q+Q_{\tau_1}}\right)}$$

provided $\mathcal{R}_{\tau_1} > \mathcal{R}_{\tau_2}$. Equations (2.20) and (2).22) reduce to the first order linear difference equation with varying coefficients

$$\begin{cases} E^-_{\tau_k} = \dfrac{H_{\tau_k} G_{\tau_{k-1}}}{H_{\tau_{k-1}}(G_{\tau_k} + H_{\tau_k} e_{\tau_k}\mathcal{R}_{c,\tau_k})} E^-_{\tau_{k-1}} + \dfrac{H_{\tau_k} F_{\tau_{k-1}} - H_{\tau_{k-1}} F_{\tau_k}}{H_{\tau_{k-1}}(G_{\tau_k} + H_{\tau_k} e_{\tau_k}\mathcal{R}_{c,\tau_k})}, \quad \text{for} \quad k = 2, 3, \ldots, r-1, \\ E^-_{\tau_r} = \dfrac{G_{\tau_{r-1}}}{e_{\tau_r}\mathcal{R}_{c,\tau_r} H_{\tau_{r-1}}} E^-_{\tau_{r-1}} + \dfrac{F_{\tau_{r-1}} - \mu H_{\tau_{r-1}}}{e_{\tau_r}\mathcal{R}_{c,\tau_r} H_{\tau_{r-1}}}. \end{cases} \tag{2.23}$$

If condition (2.18) is satisfied, then

$$\begin{aligned} \mathcal{R}_{c,\tau_{k-1}} &> \mathcal{R}_{c,\tau_k} > \frac{(Q_{\tau_{k+1}} - Q_{\tau_{k-1}})\mathcal{R}_{c,\tau_{k-1}}\mathcal{R}_{c,\tau_{k+1}}}{(Q_{\tau_{k+1}} - Q_{\tau_k})\mathcal{R}_{c,\tau_{k+1}} + (Q_{\tau_k} - Q_{\tau_{k-1}})\mathcal{R}_{c,\tau_{k-1}}}, \quad \text{for} \quad k = 2, 3, \ldots, r-1, \\ \mathcal{R}_{c,\tau_r} &> \frac{\mathcal{R}_{c,\tau_{r-1}}}{1 + (Q_{\tau_r} - Q_{\tau_{r-1}})\mathcal{R}_{c,\tau_{r-1}}}, \end{aligned}$$

so that $H_k > 0$ for $k = 1, 2, \ldots, r-1$ and

$$\begin{aligned} G_{\tau_k} + H_{\tau_k} e_{\tau_k}\mathcal{R}_{c,\tau_k} &= e_{\tau_k}\mathcal{R}_{c,\tau_k}(\mathcal{R}_{c,\tau_k} - \mathcal{R}_{c,\tau_{k+1}}(1 - \overline{\mathcal{R}}_{c,\tau_k})) > 0, \\ H_{\tau_k} F_{\tau_{k-1}} - H_{\tau_{k-1}} F_{\tau_k} &= \mu\mathcal{R}_{c,\tau_k}((Q_{\tau_{k+1}} - Q_{\tau_k})\mathcal{R}_{c,\tau_{k+1}} + (Q_{\tau_k} - Q_{\tau_{k-1}})\mathcal{R}_{c,\tau_{k-1}})\left(\mathcal{R}_{c,\tau_k} - \frac{(Q_{\tau_{k+1}} - Q_{\tau_{k-1}})\mathcal{R}_{c,\tau_{k-1}}\mathcal{R}_{c,\tau_{k+1}}}{(Q_{\tau_{k+1}} - Q_{\tau_k})\mathcal{R}_{c,\tau_{k+1}} + (Q_{\tau_k} - Q_{\tau_{k-1}})\mathcal{R}_{c,\tau_{k-1}}}\right) > 0, \\ F_{\tau_{r-1}} - \mu H_{\tau_{r-1}} &= \mu(1 + (Q_{\tau_r} - Q_{\tau_{r-1}})\mathcal{R}_{c,\tau_{r-1}})\left(\mathcal{R}_{c,\tau_r} - \frac{\mathcal{R}_{c,\tau_{r-1}}}{1 + (Q_{\tau_r} - Q_{\tau_{r-1}})\mathcal{R}_{c,\tau_{r-1}}}\right) > 0, \end{aligned}$$

and $E^-_{\tau_k} > 0$ for $k = 1, 2, \ldots, r$. The solution of the difference equation (2.23) is

$$\begin{aligned} E^-_{\tau_2} &= \varphi_{\tau_1} E^-_{\tau_1} + \eta_{\tau_1}, \\ E^-_{\tau_k} &= \left(\prod_{j=1}^{k-1}\varphi_{\tau_j}\right) E^-_{\tau_1} + \sum_{m=2}^{k-1}\left(\prod_{j=1}^{k-m}\varphi_{\tau_{k-j}}\right)\eta_{\tau_{m-1}} + \eta_{\tau_{k-1}}, \quad \text{for} \quad k = 3, 4, \ldots, r-1, \\ E^-_{\tau_r} &= \frac{G_{\tau_{r-1}}}{e_{\tau_r}\mathcal{R}_{c,\tau_r} H_{\tau_{r-1}}} E^-_{\tau_{r-1}} + \frac{F_{\tau_{r-1}} - \mu H_{\tau_{r-1}}}{e_{\tau_r}\mathcal{R}_{c,\tau_r} H_{\tau_{r-1}}}. \end{aligned}$$

Remark 2.2.2. Theorem 2.4 gives the condition for which a population can be in an endemic state with r different variants/strains on the long run. The global stability of the equilibrium point can be proven using similar method described in (Otunuga, 2022). ■

We apply our results to analyze the number of infection cases for the Covid-19 variants and lineages in Section 3.

3. Results: Covid-19 data analysis

We apply model (2.1) to analyze the number of infection cases for each of the COVID-19 variant of concern (VOC), variant of interest (VOI), or variant being monitored (VBM) by the U.S. government SARS-CoV-2 Interagency Group (SIG) nationally and for the ten U.S. Department of Health and Human Services (HHS) regions. The states and territories in each of the ten HHS regions are reported in Table 3. The daily COVID-19 cases data for each of these states and territories are available on the CDC's website (Centers for Disease Control and Prevention (CDC), 2022a) for the COVID-19 periods January 04, 2020 to 12/24/2022 and collected on 12/25/2022. These data are collected through a data supply chain. Hospitals, health care providers, laboratories first transfer case data to their respective state, local, and territorial public health departments. These departments then send the data to CDC and monitored through a surveillance systems including respiratory disease surveillance, syndromic surveillance, lab reporting, etc. Due to these surveillance systems, we assume in this study that these cases represent symptomatic cases. The total weekly COVID-19 cases for each of the ten HHS regions in the United States and nationally are shown in Fig. 4. The weekly variant proportions (Centers for Disease Control and Prevention (CDC), 2022b) for each of the ten HHS regions (and nationally) are also available online on CDC's website and are estimated nationally based on genomic sequences obtained through CDC and tagged baseline surveillance sequencing submitted to public repositories by state, local, academic, or commercial laboratories. As stated by CDC, these proportion estimates are subject to change due to changes in previously collected specimens. The population of each region can be found on the United States Census Bureau website (Annual Population Estimates, 2020). We calculate the number of cases produced by each of the variants for each of the ten HHS regions and nationally by multiplying the weekly proportion of each variants by their corresponding number of cases. The weekly proportions of these lineages in each of the ten U.S. HHS regions and nationally are shown in Figs. 2 and 3.

As of 07/23/2022, the Omicron lineages B.1.1.529, BA.2, BA.2.12.1, BA.4, BA.5, BA.1.1 of the Omicron variant are classified as VOC in the United States while the Delta lineage B.1.617.2 is classified as VBM. More lineages (BQ.1.1, BQ.1, XBB, BF.7, BN.1,BA.5.2.6,BF.11,BA.2.75.2) were added as of 12/24/2022. We note here that other lineages like the BA.1 and BA.3 and their sublineages (except BA.1.1 and its sublineages) are aggregated with B.1.1.529. Also, BA.2 sublineages (except BA.2.12.1, BA.2.75, BA.2.75.2, BN.1, XBB and their sublineages) are aggregated with BA.2. Sublineages of BA.4 are aggregated with BA.4. Sublineages of BA.5 (except BF.7, BF.11, BA.5.2.6, BQ.1, and BQ.1.1) are aggregated with BA.5. Sublineages of XBB (except XB.1.5) are aggregated with XBB.

Certain lineages infect the population at different time intervals. For example, we see from Fig. 2 that the Omicron lineages BA.2 (aggregated with BA.2.12.1), BA.4 (aggregated with BA.4.6), and BA.5 (aggregated with BA.5.2.6) predominantly infect the population between 05/28/2022 to 10/01/2022. Also, during the period 01/22/2022 to 05/21/2022, the Delta variant B.1.617.2, Omicron variant B.1.1.529 and lineages BA.1.1 and BA.2 predominantly infect the population as shown in Fig. 2. For these reasons, we analyze the infectivity of the virus using model (2.1) with $n = 3$ for the period 05/28/2022 to 10/01/2022, and $n = 4$ for the period 01/22/2022 to 05/21/2022. The weekly proportion of each of these variants are collected from CDC and analyzed within certain time frame.

Table 3 contains the states and territories included in each of the ten HHS regions as reported on the U.S. Department of Health and Human Services website (OASH Regional Offices). The weekly cases for each of the ten regions in Fig. 4 are calculated from the daily COVID-19 cases data available on the CDC website (Centers for Disease Control and Prevention (CDC), 2022a) by adding the weekly cases for the states in each region. The national weekly trend represents the weekly cases for the entire states and territories reported by CDC in the United States.

3.1. Analysis for the period 01/22/2022 to 05/21/2022

During the period 01/22/2022 to 05/21/2022, the Delta variant B.1.617.2, Omicron variant B.1.1.529, and lineages BA.1.1 and BA.2 predominantly infect the population as shown in Fig. 2. We analyze the number of cases for these variants/lineages by setting $n = 4$ in (2.1). As discussed above, we assume the available COVID-19 cases represent symptomatic cases. In this case,

Table 3
States and territories included in each of the ten HHS regions.

Regions	States and Territories
Region 1	Connecticut, Maine, Massachusetts, New Hampshire, Rhode Island, Vermont and 10 federally recognized Tribal nations.
Region 2	New Jersey, New York, Puerto Rico, U.S. Virgin Islands and Eight Federally Recognized Tribes in the Northeast.
Region 3	Delaware, the District of Columbia, Maryland, Pennsylvania, Virginia, and West Virginia.
Region 4	Alabama, Florida, Georgia, Kentucky, Mississippi, North Carolina, South Carolina, and Tennessee.
Region 5	Illinois, Indiana, Michigan, Minnesota, Ohio, and Wisconsin.
Region 6	Arkansas, Louisiana, New Mexico, Oklahoma, and Texas and 68 Federally Recognized Tribes.
Region 7	Kansas, Iowa, Missouri, and Nebraska.
Region 8	Colorado, Montana, North Dakota, South Dakota, Utah, and Wyoming.
Region 9	Arizona, California, Hawaii, Guam, Nevada, American Samoa, CNMI, FSM, Marshall Islands, and Palau.
Region 10	Alaska, Idaho, Oregon, and Washington.

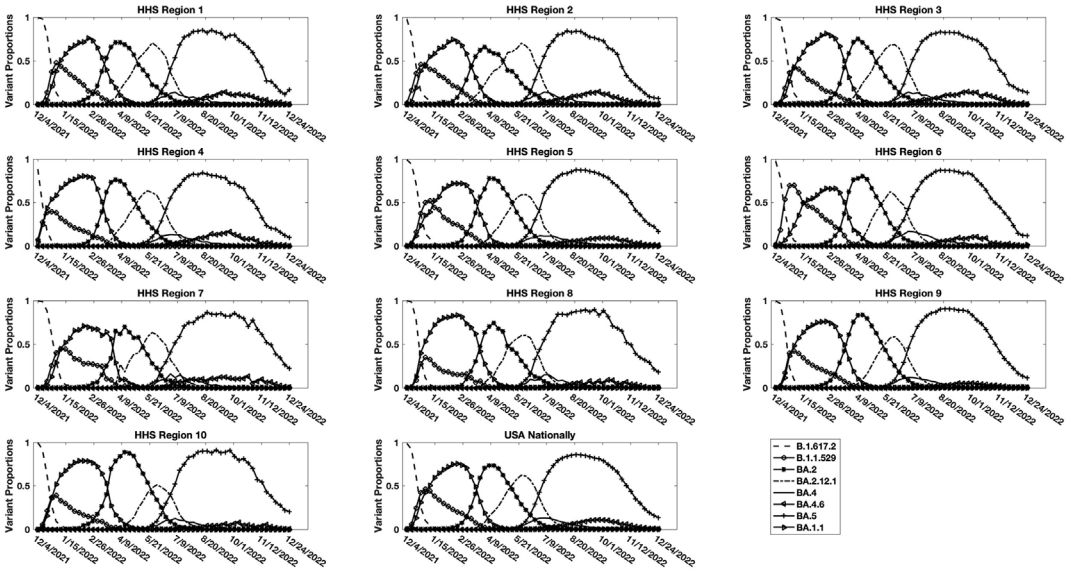

Fig. 2. Covid-19 weekly proportions by HHS regions: VOC and VBM before 07/23/2022.

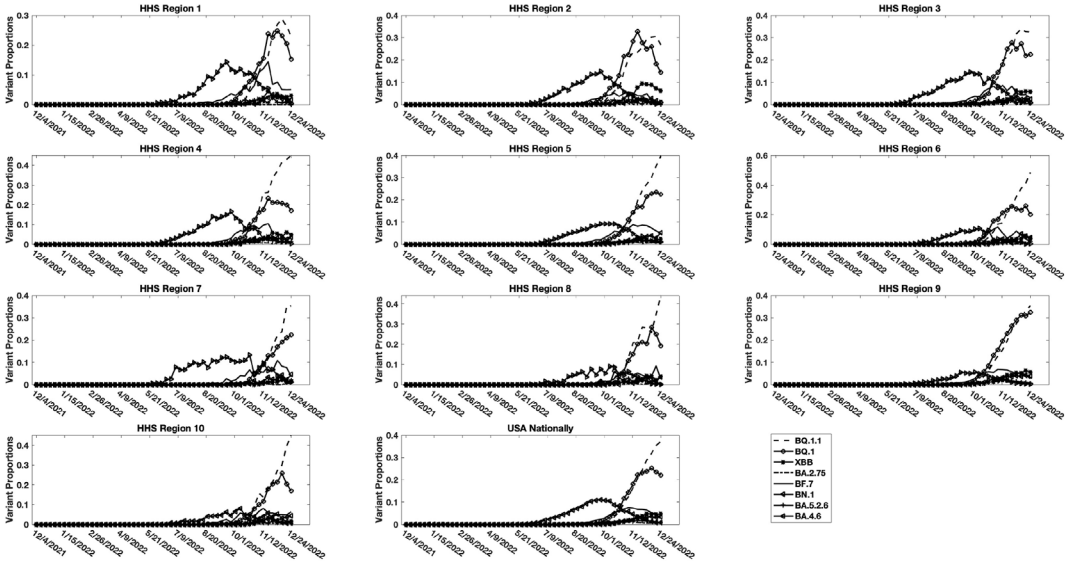

Fig. 3. Covid-19 weekly proportions by HHS regions: VOC and VBM after 07/23/2022.

the indices $j = 1, 2, 3$ and 4 denote variants B.1.617.2, B.1.1.529, BA.1.1 and BA.2, respectively. Model (2.1) is used to simulate the weekly number of infections for each of these variants for the ten HHS regions and nationally in the United States. As mentioned above, the data (referred as the real data) for I_j, $j = 1, 2, 3, 4$ is calculated by multiplying the weekly COVID-19 proportions in Fig. 2 by the weekly number of cases for each regions in Fig. 4. Denote the real and estimated weekly cases of variant j by I_j and $\hat{I}_j$, respectively. Since we only have data for I_j, $j = 1, 2, 3, 4$, parameter estimates are calculated by minimizing the sum of square error

$$SSE = \sum_{j=1}^{m} \sum_{k=1}^{n} \left(I_{k,j} - \hat{I}_{k,j} \right)^2 \tag{3.1}$$

using the Nelder-Mead simplex algorithm (Lagarias et al., 1998; Nelder & Mead, 1965), where m is the number of data points and n is the number of variants as defined in model (2.1). No published parameter is used in this analysis. That is, except for

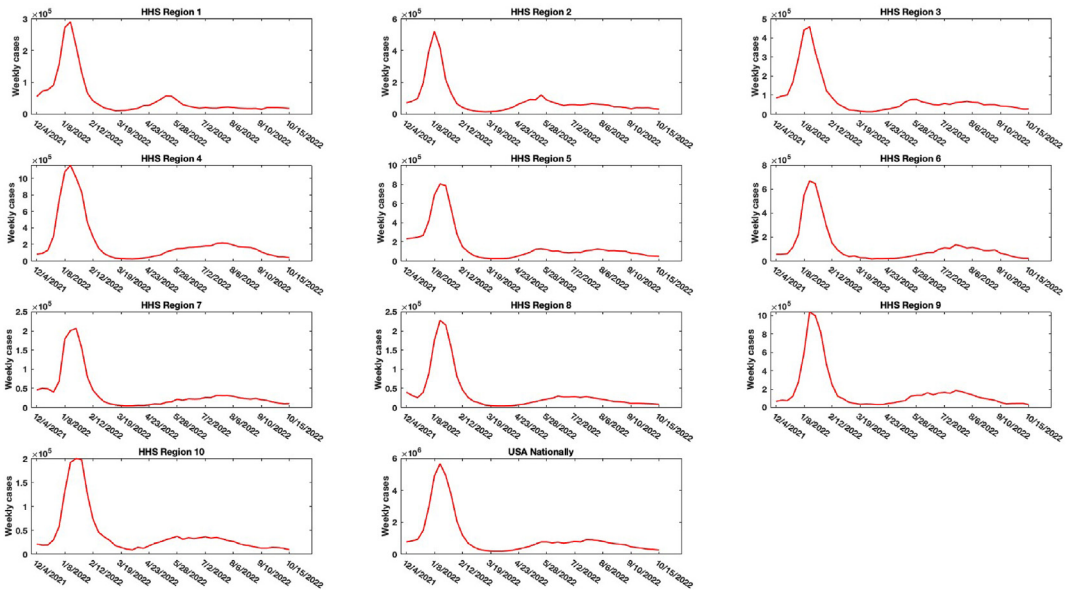

Fig. 4. Weekly trends in number of COVID-19 cases in ten HHS regions and nationally reported to CDC.

the birth/death rate μ which was assumed to be $\mu = 1/(52*77)$ since the data are weekly cases and the expected life expectancy at birth in the United States is between 76 and 78 years as of 2022, all parameters in the model are iteratively searched for by minimizing the sum of square error (3.1). This is done so as to gather as much information as possible from the estimated results. The limitation to estimating parameters in an epidemiological model using partial dataset (in this case, only data for the I_j, $j = 1, 2, 3, 4$, compartments is assumed to be known) is that the estimation algorithm is not guaranteed to converge to a local minimum. The epidemiological parameter estimates for the model (2.1) for the period 01/22/2022 to 05/21/2022 when the variants B.1.617.2, B.1.1.529, BA.1.1 and BA.2 predominantly infect the population is given in Table 4. The unit is $week^{-1}$.

Table 4
Parameter estimates for model (2.1) for each of the ten HHS regions and nationally for the period 01/22/2022 to 05/21/2022 for the variants B.1.617.2, B.1.1.529, BA.1.1 and BA.2.

Regions	Parameter Estimates															
	β_1	β_2	β_3	β_4	γ_1	γ_2	γ_3	γ_4	q_1	q_2	q_3	q_4	p_1	p_2	p_3	p_4
1	**1.0242**	**1.5693**	**0.0206**	**0.6163**	**0.1841**	**0.0173**	**0.7273**	**2.0380**	**0.0315**	**0.7119**	**0.0004**	**0.1978**	**0.7841**	**0.7357**	**0.7018**	**0.9585**
2	**0.6954**	**1.7178**	**0.0384**	**0.4680**	**0.2665**	**0.0098**	**0.7405**	**1.9232**	**0.0280**	**0.6936**	**0.0004**	**0.2583**	**0.6563**	**0.8306**	**0.7480**	**0.9613**
3	**1.3219**	**1.6340**	**0.0346**	**0.5648**	**0.2794**	**0.0103**	**0.4257**	**1.9152**	**0.0232**	**0.7003**	**0.0007**	**0.2700**	**0.6030**	**0.8274**	**0.5701**	**0.9658**
4	**0.7886**	**1.3390**	**0.0208**	**0.7665**	**0.3388**	**0.0147**	**0.3983**	**2.1213**	**0.0366**	**0.7540**	**0.0019**	**0.1912**	**0.7661**	**0.7042**	**0.3637**	**0.9508**
5	**0.4141**	**2.1962**	**0.0209**	**0.8314**	**0.1660**	**0.0095**	**0.4687**	**1.6934**	**0.0300**	**0.5175**	**0.0003**	**0.1279**	**0.6565**	**0.7556**	**0.4030**	**0.9760**
6	**0.6856**	**0.8051**	**0.0204**	**0.9124**	**0.3045**	**0.0000**	**0.3975**	**2.2620**	**0.0207**	**0.7000**	**0.0006**	**0.2700**	**0.7846**	**0.5178**	**0.3745**	**0.9847**
7	**1.1346**	**1.6723**	**0.0328**	**0.7422**	**0.2490**	**0.0114**	**0.4661**	**1.7805**	**0.0342**	**0.4329**	**0.0032**	**0.0938**	**0.9128**	**0.6165**	**0.3782**	**0.9954**
8	**0.4965**	**1.6023**	**0.0208**	**0.8811**	**0.2239**	**0.0116**	**0.4009**	**1.1543**	**0.0298**	**0.5139**	**0.0010**	**0.1975**	**0.6493**	**0.7831**	**0.3642**	**0.9618**
9	**0.7259**	**1.3834**	**0.0208**	**0.3026**	**0.2924**	**0.0091**	**0.4478**	**1.5113**	**0.0306**	**0.5334**	**0.0006**	**0.2037**	**0.7454**	**0.5059**	**0.5543**	**0.9612**
10	**1.0231**	**1.7725**	**0.0219**	**1.0140**	**0.2576**	**0.0153**	**0.9511**	**1.1730**	**0.0173**	**0.6468**	**0.0016**	**0.1211**	**0.8915**	**0.6969**	**0.3651**	**0.9720**
USA	**0.6011**	**1.1458**	**0.0244**	**0.5784**	**0.3292**	**0.0128**	**0.7565**	**2.2894**	**0.0285**	**0.6121**	**0.0009**	**0.2294**	**0.7069**	**0.7288**	**0.3639**	**0.9535**

Regions	Parameter Estimates											
	λ_1	λ_2	λ_3	λ_4	r_1	r_2	r_3	r_4	θ_1	θ_2	θ_3	θ_4
1	**0.0081**	**2.8199**	**2.7410**	**0.2164**	**0.6668**	**1.5542**	**0.5089**	**0.2072**	**1.6929**	**1.0912**	**0.5441**	**1.9793**
2	**0.0061**	**1.7046**	**1.3965**	**0.1927**	**0.6737**	**2.3749**	**0.6068**	**0.1619**	**2.2750**	**1.1033**	**0.6000**	**2.0914**
3	**0.0043**	**2.1659**	**1.9411**	**0.1698**	**0.6241**	**2.3132**	**0.9058**	**0.1685**	**1.6859**	**0.9023**	**0.4644**	**2.5595**
4	**0.0070**	**3.2991**	**2.7788**	**0.1603**	**0.7013**	**2.3500**	**0.8834**	**0.2590**	**2.3795**	**0.9325**	**0.4211**	**3.7638**
5	**0.0066**	**4.3518**	**2.6830**	**0.1838**	**0.8325**	**3.2557**	**1.1757**	**0.1568**	**3.9095**	**1.1032**	**0.4827**	**1.3176**
6	**0.0058**	**4.2230**	**2.2563**	**0.1987**	**0.7755**	**3.0302**	**0.9752**	**0.0848**	**1.7761**	**0.8278**	**0.4595**	**3.0927**
7	**0.0060**	**2.3828**	**2.4689**	**0.2575**	**1.1436**	**3.3300**	**1.1796**	**0.1797**	**1.2136**	**1.1698**	**0.4560**	**0.9976**
8	**0.0069**	**3.0953**	**2.2948**	**0.1733**	**1.3552**	**2.2543**	**1.1690**	**0.0811**	**3.2128**	**0.9286**	**0.5020**	**2.5274**
9	**0.0062**	**4.1634**	**2.7625**	**0.2195**	**0.6715**	**4.5797**	**0.9896**	**0.2285**	**2.5171**	**1.1213**	**0.4281**	**1.9868**
10	**0.0035**	**3.0965**	**2.7832**	**0.3852**	**1.2150**	**1.2399**	**1.1537**	**0.2706**	**2.9096**	**0.9236**	**0.3415**	**1.0101**
USA	**0.0090**	**3.2249**	**2.7452**	**0.1724**	**0.7912**	**3.0216**	**1.1185**	**0.2585**	**2.8652**	**0.8678**	**0.4668**	**3.1783**

Here, we see that the asymptomatic and symptomatic transmission rates of the BA.2 lineage are higher than that of the other variants B.1.617.2, B.1.1.529 and BA.1.1 for all the regions (for the period 01/22/2022 to 05/21/2022) except for regions 5, 8 and 10 where Omicron B.1.1.529 has higher symptomatic transmission rate. Also, BA.2 has the highest reproduction number compared to other variants during this period, as shown in Table 5. The variant is regarded as the "Stealth Variant" (Tiecco et al., 2022) because when compared to the original Omicron variant, it contains certain genetic traits that make it more difficult to distinguish from the Delta variant using PCR tests, thereby causing it to jump from person to person before a positive result is detected. According to Rahimi et al. (Rahimi & Abadi, 2022), the high transmissibility rate of BA.2 has enabled it to infect many individuals efficiently, explaining the high number of its positive cases. As seen in the work of Ogata (Ogata & Tanaka, 2023) and Fig. 2, the BA.2 has been the dominating strain during this period until around July 2022 when BA.5 begins to dominate. This result is in agreement with the statement made by WHO (Tiecco et al., 2022) that the BA.2 is the dominating variant during the seventh week of 2022 and it spreads faster than the BA.1 variant. The BA.2 lineage has the highest asymptomatic transmission rate in region 6 as compared to other regions, contributing to the region having the highest reproduction number. The estimates show that individuals are more vaccinated against the Omicron B.1.1.529 (as seen in the column for q_2), followed by its lineage BA.2 (as seen in the column for q_4) during this period for all the regions. The latency rate λ_1 for the Delta B.1.617.2 variant is lower than the rest of the variants for the period. This is because the Delta variant cases decline significantly than other variants during the period for all regions. Result also shows that the BA.2 lineage has a lower latency rate λ_4 compared to the B.1.1.529 and BA.1.1 lineages, with the Omicron B.1.1.529 variant having the highest latency rate. The Omicron B.1.1.529 variant has higher asymptomatic recovery rate compared to other variants in the entire regions for the specified period. Likewise, the symptomatic recovery rates for B.1.1.529 and BA.2 are higher than the others for all the regions. The latency period ($\frac{1}{e_2} weeks$) of the Omicron B.1.1.529 varies between 0.2298 week and 0.5866 week for all regions, which is equivalent to approximately 1.6–4.1 days for the time period, with the lower and upper estimate from regions 5 and 2, respectively. The latency period of the BA.1.1 variant is between 2.5 and 5 days for the time period. We see that the latency period for the BA.1.1 and BA.2 variants is lowest in region 10 than other regions. Although the estimate of the latency period for BA.2 falls outside reasonable epidemiological estimates, this might be because of its Stealth trait as discussed above. Several ranges of latency periods for different time periods and different regions have been reported in several literatures (Liu et al., 2022; Ogata & Tanaka, 2023; Tegally et al., 2022; Xin et al., 2023). The latency period estimates for Omicron B.1.1.529 and BA.1.1 fall within most of these reported intervals. The mean infectious period $\left(\frac{1}{a_2}\right.$ weeks, with interval [0.2183, 0.8064] weeks, equivalent to [1.5, 5.6] days) of asymptomatic cases is seen to be shorter than the symptomatic ($\frac{1}{w_2}$ weeks) cases (between 6 and 8.5 days) for the Omicron variant. The mean infectious period for the Delta variant appears to be shorter for the symptomatic cases (in the interval [0.2558, 0.8238] week, equivalent to [1.8, 5.8] days) than the asymptomatic cases ranging between 5 days and 11 days. The estimate for the BA.1.1 ranges between 11.7 days and 20 days for the symptomatic case and 6 days–14 days for the asymptomatic case during the same period. During this period, the mean infectious period estimate for BA.2 is between 1.9 days and 7 days for the symptomatic case but very high (3–12 weeks) for the asymptomatic case, showing that the asymptomatic case is driving the infectivity for the BA.2 variant. Estimate of the endemic equilibrium using Theorems 2.2-2.4 shows that the population is in an endemic state with BA.2 for the nation and all of the regions during this period.

The effective and basic reproduction numbers $\mathcal{R}_k$ and $\mathcal{R}_{c,k}$, respectively, for each of the variants B.1.617.2, B.1.1.529, BA.1.1 and BA.2 for the period 01/22/2022 to 05/21/2022 are given in Table 5 for the nation and the ten HHS regions. The table shows that the population is in an endemic state with the BA.2 lineage for the specified region during 01/22/2022 to 05/21/2022. Analysis in Section 3.2 for the period 05/28/2022-10/01/2022 further suggests that the population is no more in endemic state with the BA.2 lineage during this period and the lineage will eventually die out on the long run. Analysis for the period 01/22/2022-05/21/2022 shows that the Delta B.1.617.2 and Omicron B.1.1.529 variants with its lineage BA.1.1 will eventually die out on the long run. The infectivity of the lineage BA.2 is high in this period (as evidenced in its transmission rate γ_4 for all regions

Table 5
Effective and Basic Reproduction Numbers For Each HHS Regions and Nationally for the period 01/22/2022 to 05/21/2022 for the variants B.1.617.2, B.1.1.529, BA.1.1 and BA.2.

Regions	Reproduction Numbers $\mathcal{R}_k$, $k = 1,2,3$				Reproduction Numbers $\mathcal{R}_{c,k}$, $k = 1,2,3$			
	$\mathcal{R}_1$	$\mathcal{R}_2$	$\mathcal{R}_3$	$\mathcal{R}_4$	$\mathcal{R}_{c,1}$	$\mathcal{R}_{c,2}$	$\mathcal{R}_{c,3}$	$\mathcal{R}_{c,4}$
1	0.0197	0.0349	0.8128	7.5555	0.3366	0.3882	1.0137	9.4184
2	0.0069	0.0127	0.6882	8.4521	0.3502	0.2671	0.9284	11.3955
3	0.0032	0.0092	0.2187	7.9954	0.5492	0.3161	0.2998	10.9526
4	0.0070	0.0227	0.1576	6.2907	0.4321	0.4290	0.1953	7.7778
5	0.0523	0.1731	0.1625	9.1785	0.1612	0.4886	0.1864	10.5246
6	0.0033	0.0138	0.1315	19.0975	0.3750	0.4688	0.1803	26.1609
7	0.1173	0.2586	0.1753	8.9195	0.2690	0.5502	0.1941	9.8428
8	0.0402	0.1088	0.1212	10.9469	0.1558	0.3782	0.1512	13.6410
9	0.0886	0.1601	0.2167	5.0558	0.3825	0.6104	0.2724	6.3491
10	0.0452	0.1360	0.2997	3.7221	0.2120	0.5901	0.3416	4.2349
USA	0.0447	0.0569	0.2150	6.4983	0.3459	0.3610	0.2793	8.4327

in Table 4). Although the BA.2 lineage has a high transmission rate for this period, estimates also show that individuals are also recovering from the lineage at a higher rate (as evidenced in its recovery rate θ_4). An estimate of the vaccination rate q_2 suggests that high proportion of individuals are vaccinated against the Omicron B.1.1.529 variant, with an estimates r_2 and θ_2 also suggesting high recovery rates of the virus. The result of the estimate of the effective reproduction number of the Omicron B.1.1.529 and its lineages around January–February 2022, simply classified as Omicron B.1.1.529 by Liu et al. (Liu & Rocklov, 2022) shows that the effective reproduction number is in the range of 0.88 and 9.4, with a basic reproduction number in the range 5.5 and 24. Evidence showed that more lineages of the Omicron B.1.1.529 were added as of December 2021. The first case of this variant in the United States was reported on December 1, 2021. Since then, several lineages have emerged, including the BA.2 (December 21), BA.2.12.1 (December 2021 in the United States), the BA.4 (January 2022), and BA.5 (January 2022 in South Africa), which have now spread to the United States. The estimate reported by Liu is in agreement with our estimate for the BA.2 lineage. They also reported that the effective reproduction number elicited 3.8 times higher transmissibility than the Delta variant. Our estimate of the average of $\mathcal{R}_2/\mathcal{R}_1$ for the ten regions shows that the effective reproduction number of B.1.1.529 elicited 2.69 times higher transmissibility than the Delta variant.

By setting I_1, I_2, I_3 and I_4 to be the weekly COVID-19 symptomatic cases for the variants B.1.617.2, B.1.1.529, BA.1.1 and BA.2, respectively, for the period 01/22/2022 to 05/21/2022, we simulate the weekly number of infections for each of these lineages for the ten HHS regions and nationally in the United States as described in Section 3.1. The parameter estimates in Table 4 are used in the simulation process to simulate the state variables $\hat{S}, \hat{V}_j, \hat{E}_j, \hat{A}_j, \hat{I}_j, \hat{R}_j, j = 1, 2, 3$ using model (2.1), and the simulation results for $\hat{I}_j$, $j = 1, 2, 3, 4$ plotted in Figs. 5–8 for each of the regions.

3.1.1. Sensitivity index of $\mathcal{R}_k$ with respect to parameters for the variants B.1.617.2, B.1.1.529, BA.1.1 and BA.2

Although the reproduction number $\mathcal{R}_k$ helps to determine the secondary number of infections caused by an individual infected with *strain-k*, it is important to also know which epidemiological parameters in model (2.1) has the highest impact on the disease transmission and prevalence. This can be achieved using sensitivity analysis by measuring how the impact of uncertainties of one or more parameters can lead to uncertainties on the output variables. Here, we calculate the sensitivity Δ_u^F, normalized with respect to the output variable F and input variable u (Saltelli et al., 2000) and defined as $\Delta_u^F = \frac{\partial F}{\partial u} \cdot \frac{u}{F}$. This value is computed at each parameter points estimated in Table 4 for the appropriate lineages and regions. Here, F denotes the reproduction number $\mathcal{R}_k$, k=1,2,...,n, and u denotes a parameter value. A positive sensitivity index indicates that an increase in the value of the strain's parameter u leads to an increase in the basic reproduction number, $\mathcal{R}_k$. The sensitivity index of $\mathcal{R}_k$

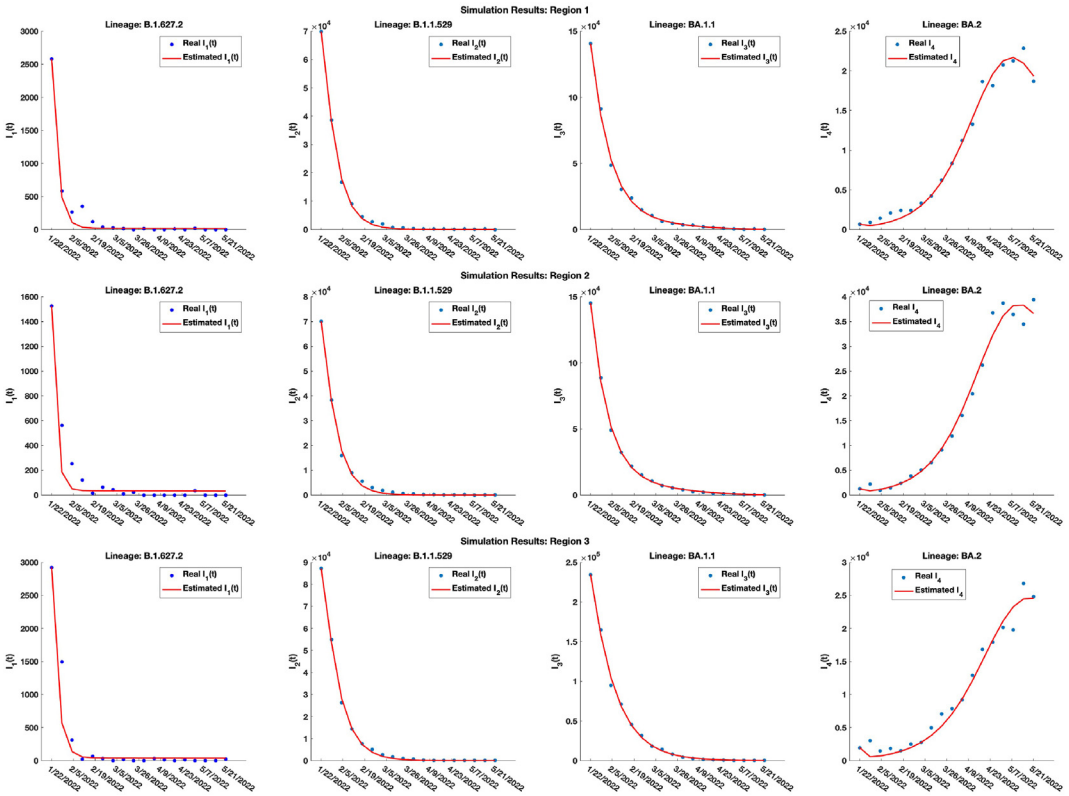

Fig. 5. Simulation results for regions 1, 2 and 3.

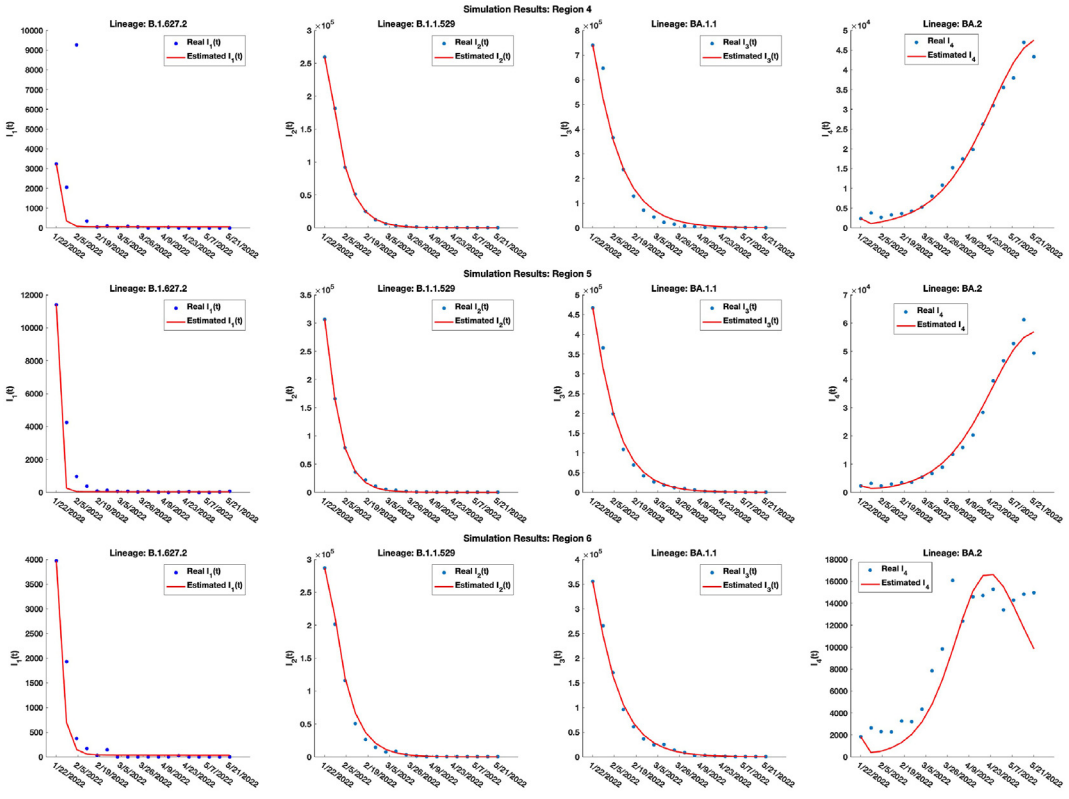

Fig. 6. Simulation results for regions 4, 5 and 6.

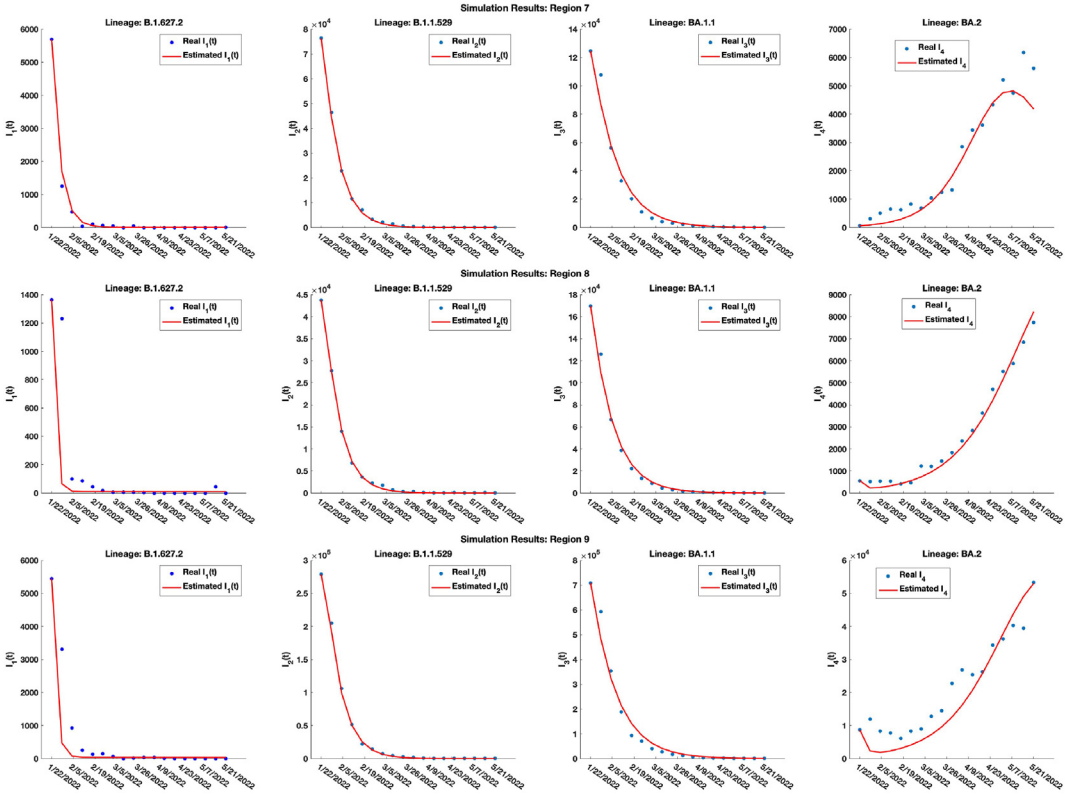

Fig. 7. Simulation results for regions 7, 8 and 9.

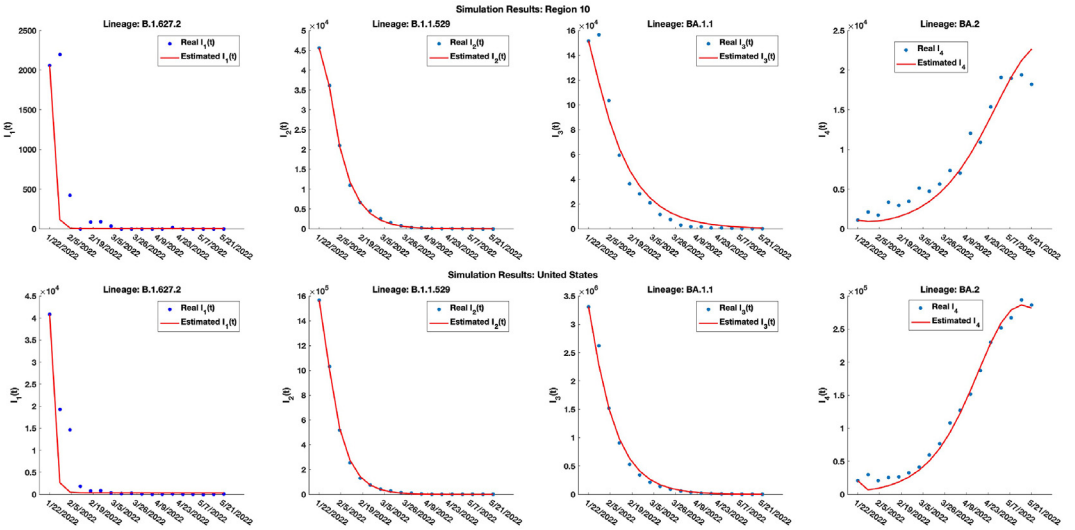

Fig. 8. Simulation Results for Region 10 and the entire nation.

with respect to each parameters u in model (2.1) is given in Table 6 for the variants B.1.617.2, B.1.1.529, BA.1.1 and BA.2 for the period 01/22/2022 to 05/21/2022. The index shows that for the Omicron lineages BA.1.1 and BA.2, the asymptomatic transmission and recovery rates have higher positive and negative impacts on the respective reproduction numbers than the symptomatic transmission and recovery rates, respectively. A similar argument applies to the Delta B.1.617.2 variant for all regions except region 3. The estimates also show that on average, the number γ_k/a_k of contacts by an infectious asymptomatic individual with others during its infectious period is less than the number β_k/w_k for a symptomatic individual for most regions for the Delta B.1.617.2 and Omicron B.1.1.529 cases since $\Delta_{p_k}^{\mathcal{R}_k} = \frac{a_k w_k p_k}{c_k}\left(\frac{\gamma_k}{a_k} - \frac{\beta_k}{w_k}\right) < 0$ for $k=1,2$. Unlike the Delta and Omicron variants, the table shows that the number is greater for an asymptomatic BA.1.1 and BA.2 cases than symptomatic case for all regions since $\Delta_{p_3}^{\mathcal{R}_3} > 0$ and $\Delta_{p_4}^{\mathcal{R}_4} > 0$. The Omicron variant has a high vaccination index $\Delta_{q_2}^{\mathcal{R}_2}$, showing the reproduction number is highly reduced due to vaccination for the period.

Table 6
Sensitivity index of $\mathcal{R}_k$ with respect to parameters u for the period 01/22/2022 to 05/21/2022 for the variants B.1.617.2, B.1.1.529, BA.1.1 and BA.2.

Regions	Sensitivity Index Δ_u^F Estimates															
u	β_1	β_2	β_3	β_4	γ_1	γ_2	γ_3	γ_4	q_1	q_2	q_3	q_4	p_1	p_2	p_3	p_4
1	**0.376**	**0.979**	**0.011**	**0.001**	**0.624**	**0.021**	**0.989**	**0.999**	**−0.539**	**−7.919**	**−0.001**	**−0.247**	**−0.743**	**−2.704**	**0.963**	**0.967**
2	**0.288**	**0.987**	**0.017**	**0.001**	**0.712**	**0.013**	**0.983**	**0.999**	**−1.421**	**−14.541**	**−0.001**	**−0.348**	**0.162**	**−4.828**	**0.931**	**0.980**
3	**0.536**	**0.988**	**0.107**	**0.001**	**0.464**	**0.012**	**0.893**	**0.999**	**−4.000**	**−24.148**	**−0.001**	**−0.370**	**−0.349**	**−4.726**	**0.752**	**0.980**
4	**0.173**	**0.990**	**0.161**	**0.001**	**0.827**	**0.010**	**0.839**	**0.999**	**−2.245**	**−14.253**	**−0.002**	**−0.236**	**0.260**	**−2.346**	**0.747**	**0.974**
5	**0.218**	**0.996**	**0.139**	**0.001**	**0.783**	**0.005**	**0.861**	**0.999**	**−0.093**	**−1.461**	**0.000**	**−0.147**	**0.367**	**−3.073**	**0.768**	**0.940**
6	**0.213**	**1.000**	**0.154**	**0.000**	**0.787**	**0.000**	**0.846**	**1.000**	**−2.379**	**−23.810**	**−0.001**	**−0.370**	**0.013**	**−1.074**	**0.754**	**0.989**
7	**0.291**	**0.996**	**0.230**	**0.000**	**0.709**	**0.004**	**0.770**	**1.000**	**−0.079**	**−0.921**	**−0.004**	**−0.104**	**−2.336**	**−1.598**	**0.630**	**0.925**
8	**0.336**	**0.989**	**0.174**	**0.001**	**0.664**	**0.011**	**0.826**	**0.999**	**−0.116**	**−1.787**	**−0.001**	**−0.246**	**0.043**	**−3.561**	**0.726**	**0.975**
9	**0.185**	**0.998**	**0.080**	**0.001**	**0.816**	**0.002**	**0.921**	**0.999**	**−0.132**	**−2.034**	**−0.001**	**−0.256**	**0.275**	**−1.021**	**0.822**	**0.976**
10	**0.168**	**0.985**	**0.119**	**0.007**	**0.832**	**0.015**	**0.881**	**0.993**	**−0.081**	**−2.806**	**−0.002**	**−0.138**	**−0.548**	**−2.251**	**0.812**	**0.763**
USA	**0.173**	**0.992**	**0.119**	**0.001**	**0.827**	**0.009**	**0.881**	**0.999**	**−0.221**	**−3.884**	**−0.001**	**−0.298**	**0.410**	**−2.656**	**0.813**	**0.979**

Regions	Sensitivity Index Δ_u^F Estimates											
u	λ_1	λ_2	λ_3	λ_4	r_1	r_2	r_3	r_4	θ_1	θ_2	θ_3	θ_4
1	**0.0299**	**0.0001**	**0.0001**	**0.0012**	**−0.6234**	**−0.0211**	**−0.9884**	**−0.9974**	**−0.3763**	**−0.9787**	**−0.0111**	**−0.0014**
2	**0.0393**	**0.0001**	**0.0002**	**0.0013**	**−0.7116**	**−0.0128**	**−0.9822**	**−0.9977**	**−0.2881**	**−0.9869**	**−0.0174**	**−0.0008**
3	**0.0549**	**0.0001**	**0.0001**	**0.0015**	**−0.4642**	**−0.0117**	**−0.8930**	**−0.9978**	**−0.5355**	**−0.9881**	**−0.1067**	**−0.0007**
4	**0.0344**	**0.0001**	**0.0001**	**0.0016**	**−0.8265**	**−0.0103**	**−0.8390**	**−0.9978**	**−0.1732**	**−0.9895**	**−0.1607**	**−0.0013**
5	**0.0365**	**0.0001**	**0.0001**	**0.0014**	**−0.7822**	**−0.0045**	**−0.8613**	**−0.9970**	**−0.2175**	**−0.9953**	**−0.1385**	**−0.0014**
6	**0.0413**	**0.0001**	**0.0001**	**0.0013**	**−0.7872**	**0.0000**	**−0.8459**	**−0.9969**	**−0.2125**	**−0.9997**	**−0.1538**	**−0.0002**
7	**0.0400**	**0.0001**	**0.0001**	**0.0010**	**−0.7090**	**−0.0038**	**−0.7695**	**−0.9983**	**−0.2908**	**−0.9960**	**−0.2302**	**−0.0003**
8	**0.0349**	**0.0001**	**0.0001**	**0.0014**	**−0.6642**	**−0.0107**	**−0.8257**	**−0.9960**	**−0.3356**	**−0.9891**	**−0.1741**	**−0.0010**
9	**0.0387**	**0.0001**	**0.0001**	**0.0011**	**−0.8152**	**−0.0016**	**−0.9203**	**−0.9980**	**−0.1845**	**−0.9981**	**−0.0794**	**−0.0009**
10	**0.0666**	**0.0001**	**0.0001**	**0.0006**	**−0.8319**	**−0.0146**	**−0.8807**	**−0.9925**	**−0.1680**	**−0.9852**	**−0.1190**	**−0.0066**
USA	**0.0270**	**0.0001**	**0.0001**	**0.0014**	**−0.8268**	**−0.0085**	**−0.8808**	**−0.9980**	**−0.1729**	**−0.9912**	**−0.1189**	**−0.0010**

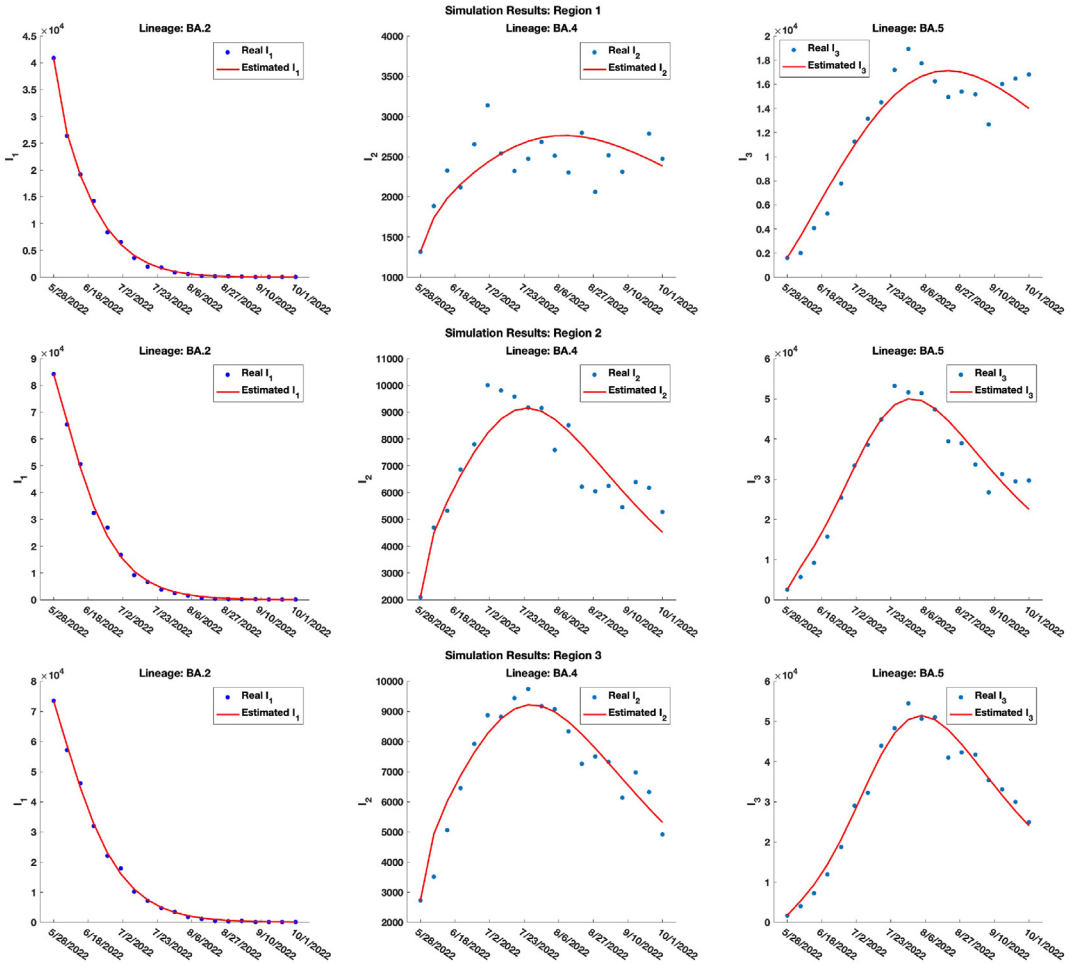

Fig. 9. Simulation results for regions 1, 2 and 3.

3.2. Analysis for the period 05/28/2022 to 10/01/2022

As shown in Figs. 2–3, the Omicron lineages BA.2,[1] BA.4 ,[2] and BA.5 [3] predominantly infect the population between 05/28/2022 to 10/01/2022. For the rest of this section, a mention of BA.2, BA.4, and BA.5 (in addition to the discussion in Section 3) means BA.2 aggregated with BA.2.12.1, BA.4 aggregated with BA.4.6, and BA.5 aggregated with BA.5.2.6, respectively. For this reason, we shall denote these lineages by BA.2*, BA.4*, and BA.5* instead of BA.2, BA.4, and BA.5 in this section. We analyze the number of cases for these lineages using model (2.1) by setting $n = 3$. In this case, the indices $j = 1, 2$ and 3 denote variants BA.2*, BA.4* and BA.5*, respectively. We assume the weekly COVID-19 cases for the Omicron lineages BA.2*, BA.4*, BA.5* are symptomatic cases denoted by I_1, I_2, and I_3, respectively, for the period 05/28/2022 to 10/01/2022. As mentioned earlier, the data (referred as the real data) for I_1, I_2, and I_3 is calculated by multiplying the weekly COVID-19 proportions in Fig. 2 by the weekly number of cases in Fig. 4. These cases are assumed to satisfy model (2.1) and estimated by iteratively searching for parameters that minimized the sum of square errors (3.1) using the Nelder-Mead simplex algorithm (Lagarias et al., 1998; Nelder & Mead, 1965) for the nation and each of the ten HHS regions in the United States. The simulation results for $\hat{I}_j, j = 1, 2, 3$, for each HHS regions are plotted in Figs. 9–12. Note that in these figures, the lineages BA.2, BA.4, and BA.5 mean BA.2*, BA.4*, and BA.5*.

Table 7 contains parameter estimates for each of the ten HHS regions and the United States as a nation using model (2.1) for the period between 05/28/2022 to 10/01/2022 where the Omicron lineages BA.2*, BA.4*, BA.5* predominantly infect the population. Here, indices 1, 2, and 3 represent the Omicron lineages BA.2*, BA.4*, and BA.5*, respectively. We set $\mu = 1/$

[1] (aggregated with BA.2.12.1).
[2] (aggregated with BA.4.6).
[3] (aggregated with BA.5.2.6).

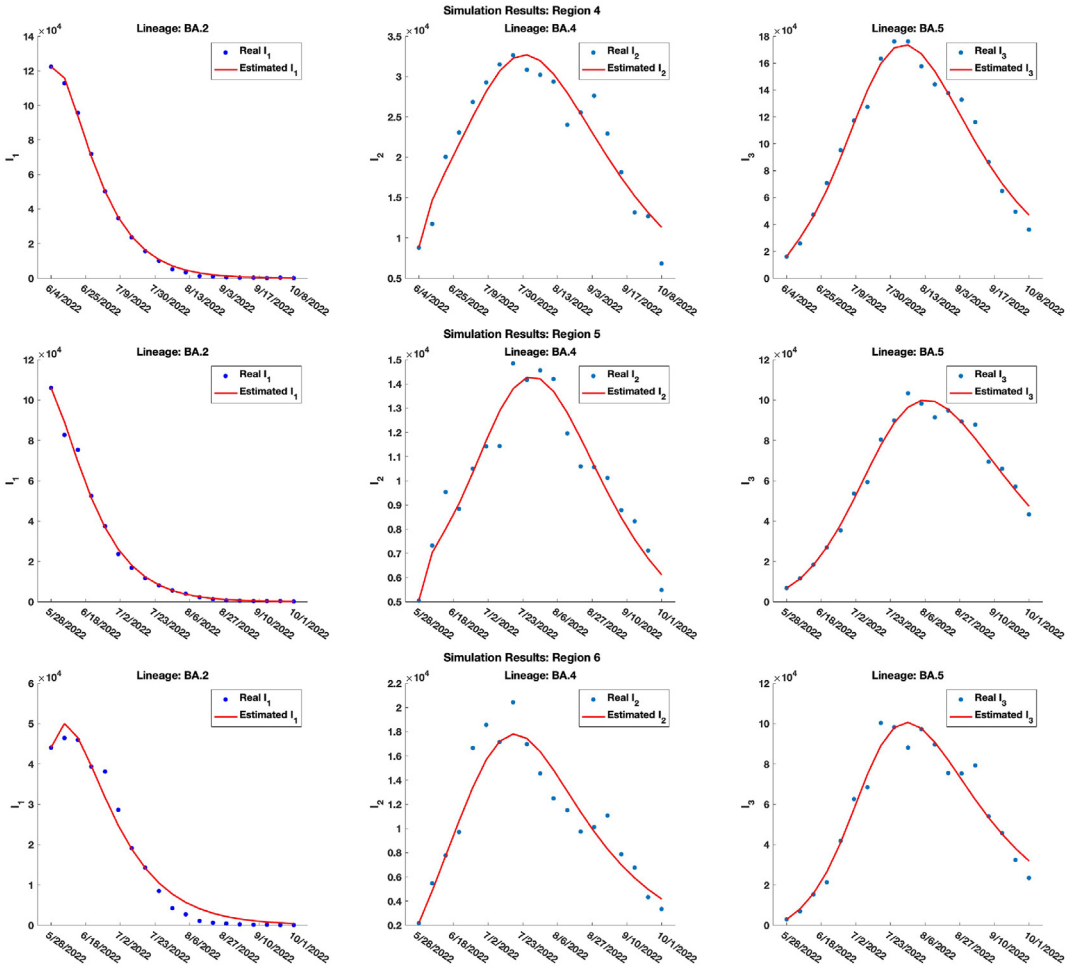

Fig. 10. Simulation results for regions 4, 5 and 6.

(52*77). The unit of the parameters is $week^{-1}$. The mean latency period ($\frac{1}{e_k}$ weeks) of the BA.2* lineage is higher than that of BA.4* and BA.5* during this period (except in region 1), showing that it takes longer for an individual infected by the lineage to become infectious during the period. The symptomatic mean infectious period $\left(\frac{1}{a_k} \text{ weeks}\right)$ for the lineage is the lowest in all regions and the asymptomatic mean infectious period lowest in most regions (except regions 1,4,8,10). This is equivalent to high recovery rates in the regions mentioned. This probably explains one of the reasons why the lineage dies off during the period. As seen in earlier analysis of the lineage's transmissibility in Table 4 and the work of Ogata (Ogata & Tanaka, 2023), the BA.2* has been the dominating strain around March 2022 until around July 2022 when BA.5* begins to dominate. The asymptomatic and symptomatic transmission rates of BA.5* is greater than that of BA.2* and BA.4* in the nation as seen in the last row of Table 7. Likewise, the symptomatic and asymptomatic transmission rates are higher in several regions like regions 2,3,7,8,10 and 1,3,4,5,8,10, respectively. The asymptomatic and symptomatic transmission rates of the BA.4* lineage is also higher than the others in some regions. The BA.4* has a higher asymptomatic mean infectious period than the BA.5* lineage in regions (except in regions 6,7,9). The BA.4* (BA.5*) has a lower mean latency period than BA.2* in the nation and all regions except region 1. They both have a higher symptomatic mean infectious period than the BA.2* lineage. Their high infectivity during this period could be as a result of their low Neutralizing antibody titers, as measured in the work of Hachmann et al. (Hachmann et al., 2022). They measured the neutralizing antibody titers against the SARSCoV-2 strain and against omicron subvariants BA.1, BA.2, BA.4, BA.5, and BA.4.6 in participants who had been vaccinated and boosted with the original mRNA-1273 vaccine (Moderna) and noticed that the BA.4.6 omicron subvariant markedly escaped neutralizing antibodies induced by infection or vaccination with lower value than the rest of the variants, followed by the BA.4-BA.5 variants. This result is also confirmed in the work of He (He et al., 2020).

The mean symptomatic infectious period for BA.2*, BA.4*, and BA.5* cases for all regions are estimated to be in the interval (0.6, 3) weeks, (2.5, 6.5) weeks, and (3.8, 8.0) weeks, respectively. Likewise, the mean infectious period for the asymptomatic BA.2*, BA.4*, and BA.5* cases for all regions are estimated to be in the interval (0.1, 3.7) weeks, (0.4, 9.4) weeks, and (0.3, 2.3)

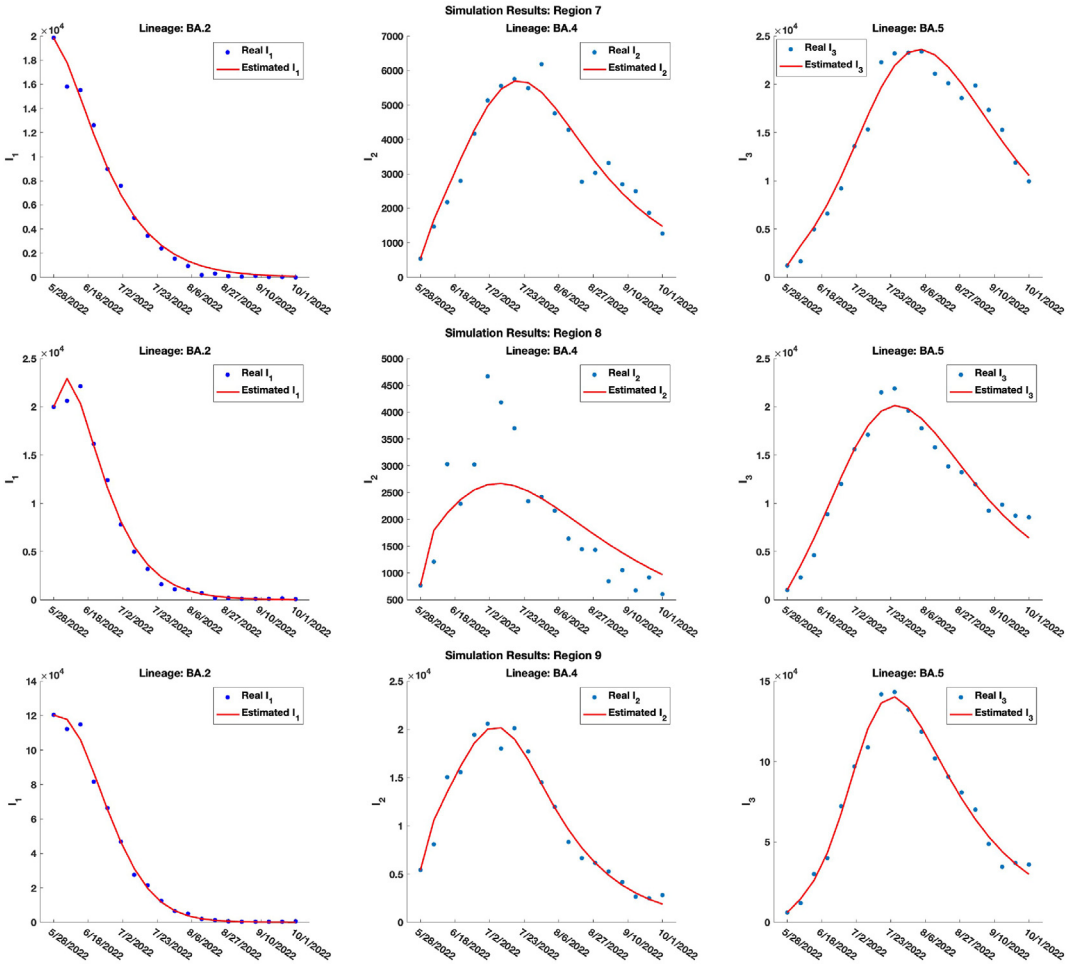

Fig. 11. Simulation results for regions 7, 8 and 9.

weeks, respectively. The mean latency periods for BA.2*, BA.4*, and BA.5* are calculated to be in the interval (0.9, 2.3) weeks, (0.2, 1.4) weeks, and (0.2, 1.6) weeks, respectively, for all regions. Nationally, the mean latency period of BA.2*, BA.4*, and BA.5* for the period is 2, 0.75, and 0.85 weeks, respectively, showing that individuals exposed to BA.4*, and BA.5* become infectious within a shorter days during the period.

Table 8 also shows the estimate for the reproduction numbers derived in (2.6) for each of the ten HHS regions for the period 05/28/2022 to 10/01/2022 and for the lineages BA.2*, BA.4*, and BA.5*. The subscripts $j = 1, 2, 3$ in the reproduction numbers $\mathcal{R}_1$, $\mathcal{R}_2$ and $\mathcal{R}_3$ in Table 8 denote that of BA.2*, BA.4*, and BA.5*, respectively. The national reproduction numbers for the BA.2*, BA.4*, and BA.5* as of 05/28/2022 to 10/01/2022 are calculated to be approximately 0.18, 1.99 and 2.63, respectively, in Table 8 (last row), showing that the BA.5* lineage has the highest reproduction number, nationally. The table also shows that the BA.5* lineage has the highest effective reproduction number in all except regions 1 and 5 while BA.4* has the second highest effective reproduction number in all regions except regions 1 and 5 where it has the highest number. The higher reproduction number for BA.5* supports the higher number of cases of the lineage as compared with other lineages in the same period. The comparison of the estimates of $\mathcal{R}_k$ and $\mathcal{R}_{c,k}$, $k = 1, 2, 3$, in Table 8 suggests vaccination is more effective in the reduction in number of infections against BA.2*, BA.4*, and BA.5*, with the highest effect seen in BA.2*. This is also confirmed in the work of Kislaya et al. (Kislaya et al., 2023) who stated that although booster vaccination is less effective against BA.5 than against BA.2, it offers significant protection against the progression from BA.5 infection to severe disease. Also, Dhawan et al. (Dhawan et al., 2022) confirms the effectiveness of the first two doses of vaccines in reducing the worst clinical outcomes and hospitalization admissions, while a third or booster dose significantly provides additional protection to overcome the reduced neutralization associated with the Omicron variants. Estimate of the endemic equilibrium using Theorems 2.2-2.4

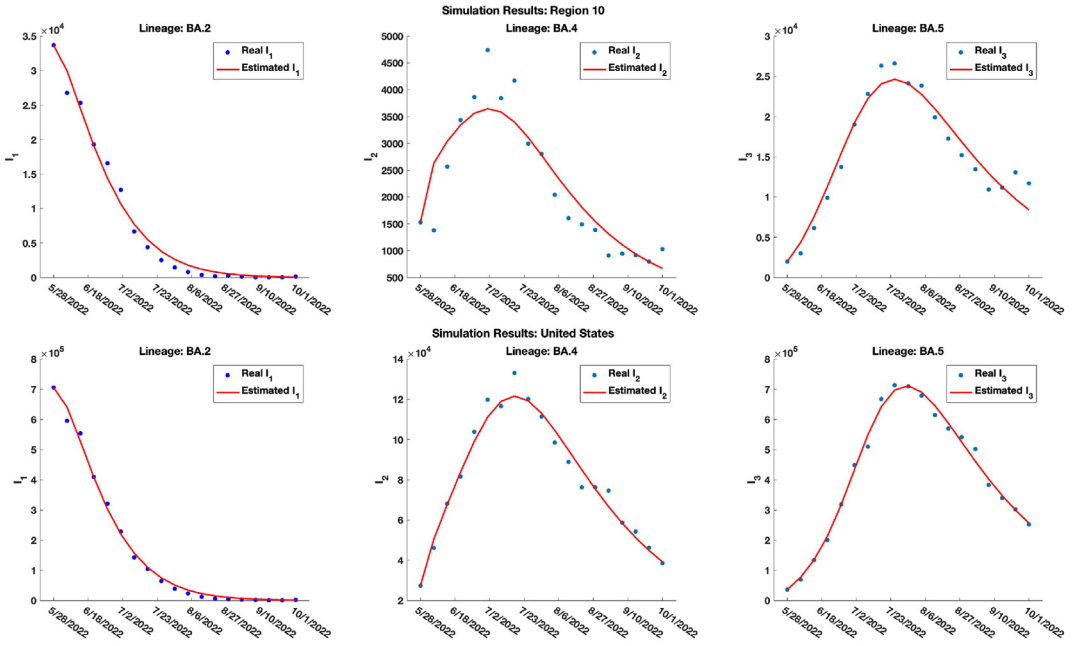

Fig. 12. Simulation Results for Region 10 and the entire nation.

shows that the population is in an endemic state with BA.5* for the nation and most of the regions except in regions 1,3 and 5 where the population is in endemic state with BA.4* and BA.5* during this period.

3.2.1. Sensitivity analysis

Here, we calculate the sensitivity Δ_u^F, normalized with respect to the output variable F and input variable u (Saltelli et al., 2000). This value is computed at each parameter points estimated in Table 7 for the appropriate lineages and regions. Here, F denotes the reproduction number $\mathcal{R}_k$, $k = 1, 2, \ldots, n$ and u denotes a parameter value. The sensitivity index of $\mathcal{R}_k$ with respect to each parameters u in model (2.1) is given in Table 9.

The sensitivity index $\Delta_{p_k}^{\mathcal{R}_k}$ of $\mathcal{R}_k$, $k = 1, 2, 3, \ldots, n$, with respect to p_k is obtained as

$$\Delta_{p_k}^{\mathcal{R}_k} = \frac{a_k w_k p_k}{c_k}\left(\frac{\gamma_k}{a_k} - \frac{\beta_k}{w_k}\right).$$

The index $\Delta_{p_k}^{\mathcal{R}_k} > 0$ if on average, the number γ_k/a_k of contacts by an infectious asymptomatic individual with others during its infectious period is greater than the number β_k/w_k for a symptomatic individual so that an increase in the proportion of the asymptomatic cases will result in an increase in the effective reproduction number. The estimate $\Delta_{p_2}^{\mathcal{R}_2}$ in Table 9 shows that on the average, the number of contacts by an infectious BA.4* asymptomatic individual during its infectious period is less than that for a symptomatic individual for regions 2, 3, 4, 6, 9. This also supports the reason why the asymptomatic mean infectious period is lower than that of the symptomatic case, as analyzed in the previous section. Likewise, the number of contacts by one BA.2* (BA.5*) asymptomatic infectious individual during its infectious period is lesser than that produced by a symptomatic infectious individual for the entire region except in regions 1, 3, 4, 6, 8, 9 (regions 6, 9) where an increase in the proportion of the asymptomatic cases results in an increase in reproduction number. This analysis shows, as explained in the work of He et al. (He et al., 2020), that the transmissibility (of an infectious disease) of the asymptomatic and symptomatic cases varies based on the disease, and it can be quantified by the reproduction number. The table shows that for the BA.4* and BA.5* lineages in all regions, the asymptomatic transmission rate γ_k has higher positive impact on the reproduction number $\mathcal{R}_k$ than the symptomatic transmission rate β_k for $k = 2, 3$ (even though $\beta_2 > \gamma_2$ in regions 2, 3 and $\beta_3 > \gamma_3$ in regions 2, 7, 10 on Table 7). This is because $\frac{\Delta_{\gamma_k}^{\mathcal{R}_k}}{\Delta_{\beta_k}^{\mathcal{R}_k}} = \frac{p_k\gamma_k/a_k}{(1-p_k)\beta_k/w_k} > 1$, $k = 2, 3$ for all regions. A similar argument applies to the BA.2* lineage except in region 10. Likewise, the asymptomatic recovery rate r_3 for BA.5* has higher negative impact on the reproduction number $\mathcal{R}_3$ than the symptomatic recovery rate θ_3 for all regions. The same can be said about the BA.2* and BA.4* lineages except in regions 10 and 2, respectively. The table also shows that the latency rate λ_k has positive impact on the reproduction number for all variants and regions, as expected.

Table 7
Parameter estimates for model (2.1) for each of the ten HHS regions and nationally for the period 05/28/2022 to 10/01/2022 for the Omicron lineages BA.2*, BA.4*, and BA.5*.

Regions	Parameter Estimates																				
	β_1	β_2	β_3	γ_1	γ_2	γ_3	q_1	q_2	q_3	p_1	p_2	p_3	λ_1	λ_2	λ_3	r_1	r_2	r_3	θ_1	θ_2	θ_3
1	**3.1141**	**0.1424**	**0.6889**	**3.7475**	**0.9237**	**6.4021**	**0.3177**	**0.0114**	**0.3019**	**0.5097**	**0.6639**	**0.9897**	**1.1398**	**0.7389**	**0.7952**	**1.8912**	**0.3160**	**3.5438**	**1.7203**	**0.2874**	**0.1257**
2	**0.7731**	**1.9473**	**7.6043**	**5.6217**	**1.1659**	**2.2850**	**0.3278**	**0.0762**	**0.3328**	**0.9426**	**0.8123**	**0.9895**	**0.4965**	**2.6045**	**4.4602**	**7.3156**	**0.9035**	**1.1038**	**0.7137**	**0.2142**	**0.1940**
3	**0.6842**	**1.1571**	**2.4479**	**1.6796**	**0.9898**	**2.7391**	**0.2376**	**0.2237**	**0.2974**	**0.9127**	**0.8020**	**0.9900**	**0.5060**	**1.5683**	**2.8047**	**1.5731**	**0.4510**	**1.2793**	**0.7082**	**0.1668**	**0.1828**
4	**0.9390**	**1.3112**	**1.1227**	**1.5902**	**1.9383**	**2.4812**	**0.2298**	**0.2138**	**0.3474**	**0.9731**	**0.8333**	**0.9856**	**0.6121**	**1.2492**	**1.1581**	**0.2679**	**0.3206**	**0.5995**	**0.5234**	**0.2167**	**0.2659**
5	**2.0961**	**0.5825**	**1.0648**	**2.4334**	**1.0830**	**3.5607**	**0.4255**	**0.0822**	**0.3623**	**0.8650**	**0.6751**	**0.9897**	**0.4645**	**1.0996**	**0.6156**	**3.5024**	**0.1060**	**0.9671**	**0.5883**	**0.4032**	**0.2102**
6	**0.0407**	**3.3066**	**0.2500**	**1.6022**	**4.1320**	**4.0451**	**0.1370**	**0.0059**	**0.2785**	**0.9360**	**0.9725**	**0.9895**	**0.6078**	**1.1188**	**1.4667**	**9.6339**	**2.3220**	**1.6020**	**0.3326**	**0.2078**	**0.1932**
7	**0.2066**	**0.1189**	**9.7038**	**0.5570**	**3.9480**	**1.7370**	**0.0189**	**0.1650**	**0.3468**	**0.8726**	**0.7279**	**0.9894**	**0.4329**	**4.2325**	**3.1439**	**2.2501**	**1.0851**	**0.7220**	**0.5016**	**0.1799**	**0.2178**
8	**0.8884**	**0.0069**	**2.2108**	**2.4611**	**1.4299**	**3.3139**	**0.3867**	**0.0315**	**0.3568**	**0.6701**	**0.8115**	**0.9898**	**1.0335**	**1.3001**	**2.7257**	**1.0721**	**0.6011**	**1.4268**	**0.5520**	**0.1546**	**0.1905**
9	**1.2010**	**1.2164**	**0.1370**	**3.8539**	**1.4120**	**2.2410**	**0.0499**	**0.0934**	**0.3359**	**0.9467**	**0.7197**	**0.9899**	**0.7656**	**2.0312**	**1.8320**	**2.0886**	**0.4741**	**0.4319**	**0.8644**	**0.2541**	**0.2110**
10	**2.6279**	**0.1345**	**7.2094**	**0.0626**	**3.4774**	**5.3077**	**0.0210**	**0.1161**	**0.5208**	**0.7973**	**0.4206**	**0.9898**	**0.5444**	**1.8174**	**1.0340**	**1.1127**	**0.2693**	**1.3380**	**0.5911**	**0.3123**	**0.1703**
USA	**1.4439**	**1.0732**	**4.3087**	**1.8242**	**1.5548**	**3.4608**	**0.2979**	**0.0000**	**0.5201**	**0.8325**	**0.7737**	**0.9886**	**0.5002**	**1.3386**	**1.1711**	**2.7515**	**0.4638**	**0.6595**	**0.5313**	**0.1556**	**0.1719**

Table 8
Effective and Basic Reproduction Numbers For Each HHS Regions and Nationally for the period 05/28/2022 to 10/01/2022 for the Omicron lineages BA.2*, BA.4*, and BA.5*.

Regions	$\mathcal{R}_k,\ k=1,2,3$			$\mathcal{R}_{c,k},\ k=1,2,3$		
	$\mathcal{R}_1$	$\mathcal{R}_2$	$\mathcal{R}_3$	$\mathcal{R}_{c,1}$	$\mathcal{R}_{c,2}$	$\mathcal{R}_{c,3}$
1	0.7001	1.4453	1.2871	1.8969	2.1046	1.8437
2	0.2068	1.6262	1.6395	0.7861	2.7518	2.4574
3	0.2553	1.4993	1.5828	1.0581	3.1305	2.2528
4	1.2157	2.6505	2.7000	5.8166	6.0404	4.1373
5	0.1406	4.0822	2.3554	1.0812	7.3487	3.6936
6	0.0946	1.5507	1.8119	0.1634	2.1670	2.5113
7	0.1259	1.3802	1.8623	0.2683	2.8272	2.8510
8	0.4652	1.1852	1.5545	2.0681	1.9378	2.4169
9	0.9479	1.9874	3.4129	1.8201	3.4824	5.1392
10	0.3233	2.0605	2.0873	0.9452	5.6746	4.3558
USA	0.1832	1.9915	2.6250	1.0064	4.1498	5.4700

4. Summary and conclusion

Since the year 2020, the spread of all variants of the COVID-19 virus is being tracked and monitored by health officials in the United States and around the world. During the early stage of the spread of the virus infection, public health officials believe certain vaccines can prevent the virus infection and those who recovered from the virus are safe from being reinfected. Current studies show that the current circulating variant (Omicron) and its lineages can spread from anyone with the infection to others, regardless of their vaccination or recovery status. In this study, we construct a model suitable for describing the spread of a virus for a scenario where there is a vaccine breakthrough infection and rebound infection. The model is used to estimate epidemiological metrics such as the effective and basic reproduction numbers for the Delta B.1.617.2, Omicron B.1.1.529, and lineages BA.2, BA.2.12.1, BA.2*, BA.4*, BA.5*, BA.1.1, BA.4.6, and BA.5.2.6 for the United States and for each of the ten HHS regions in the United States for the periods 01/22/2022-05/21/2022 and 05/28/2022-10/01/2022 when certain lineages are dominating. The epidemiological parameters in the constructed model are also estimated and used to describe the infectivity of the variants/lineages in each of the regions. Our analysis shows that the BA.2 lineage of Omicron infects more individuals than other lineage during the infection period 01/22/2022-05/21/2022 for all the ten regions and the nation, as evidenced in its reproduction numbers reported in Table 5. The lineage also has a low asymptomatic recovery rate compared to others for all regions and the nation during this period. The Omicron variant B.1.1.529 and lineage BA.2 have the highest symptomatic and asymptomatic transmission rates, respectively, for all regions for the period. Likewise, the Omicron variant B.1.1.529 has the highest asymptomatic recovery rates compared to other variants. The sensitivity analysis of dominating variants in the period shows that the transmission γ_4 and recovery r_4 rates for the BA.2 lineage contribute highly positively and negatively, respectively, to the number of infections produced by the virus. The virus also has a high vaccination index $\Delta_{q_2}^{\mathcal{R}_2}$ for Omicron for the period. Further analysis on the predominant variants/lineages in the period 05/28/2022-10/01/2022 shows that the BA.5* lineage of Omicron has the highest asymptomatic transmission rate in the nation and in every region except regions 2, 6, 7, 9, and highest symptomatic transmission rate in the nation and in regions 2, 3, 7, 8, 10. Its reproduction number, calculated on Table 8, shows that the lineage has the highest number of secondary infections in all regions except regions 1, 5. The sensitivity index analysis for the variant shows that the asymptomatic transmission rate γ_3 has higher positive impact on the reproduction number $\mathcal{R}_3$ than the symptomatic transmission rate β_3. A similar argument applies to the BA.4* lineage in all regions and the BA.2* lineage in all region except region 10. The comparison of the estimates of the effective and basic reproduction numbers in Table 8 suggests that vaccination is more effective in the reduction of the number of BA.2*, BA.4*, and BA.5* infections, with the highest effect seen in BA.2*. We state here that the analysis presented in this work are all based on the estimates of the epidemiological parameters and metrics produced by assuming the number of Covid-19 cases satisfy model (2.1). This research is still ongoing and more assumptions are tested as more data are available and more lineages emerge.

Table 9
Sensitivity index of $\mathcal{R}_k$ with respect to each parameters u for the period 05/28/2022 to 10/01/2022 for the Omicron lineages BA.2*, BA.4*, and BA.5*.

Regions u	Sensitivity Index Δ_u^F Estimates																			
	β_1	β_2	β_3	γ_1	γ_2	γ_3	q_1	q_2	q_3	p_1	p_2	p_3	λ_1	λ_2	λ_3	r_1	r_2	r_3	θ_1	θ_2	θ_3
1	**0.4677**	**0.0790**	**0.0306**	**0.5323**	**0.9210**	**0.9694**	**−0.8607**	**−0.0166**	**−0.4325**	**0.0460**	**0.7649**	**−1.9653**	**0.0002**	**0.0003**	**0.0003**	**−0.5322**	**−0.9203**	**−0.9693**	**−0.4676**	**−0.0789**	**−0.0306**
2	**0.0791**	**0.6192**	**0.1666**	**0.9209**	**0.3808**	**0.8334**	**−1.2460**	**−0.1290**	**−0.4989**	**−0.3769**	**−2.2995**	**−14.9304**	**0.0005**	**0.0001**	**0.0001**	**−0.9209**	**−0.3807**	**−0.8332**	**−0.0790**	**−0.6185**	**−0.1664**
3	**0.0797**	**0.4381**	**0.0593**	**0.9203**	**0.5619**	**0.9407**	**−0.9847**	**−0.4670**	**−0.4233**	**0.0876**	**−1.2125**	**−4.9350**	**0.0005**	**0.0002**	**0.0001**	**−0.9202**	**−0.5615**	**−0.9405**	**−0.0797**	**−0.4375**	**−0.0593**
4	**0.0083**	**0.1668**	**0.0147**	**0.9917**	**0.8332**	**0.9853**	**−1.0995**	**−0.4872**	**−0.5323**	**0.6918**	**−0.0004**	**−0.0193**	**0.0004**	**0.0002**	**0.0002**	**−0.9908**	**−0.8326**	**−0.9849**	**−0.0083**	**−0.1666**	**−0.0147**
5	**0.4445**	**0.0638**	**0.0141**	**0.5555**	**0.9362**	**0.9859**	**−3.2731**	**−0.1480**	**−0.5681**	**−2.2923**	**0.8036**	**−0.3693**	**0.0005**	**0.0002**	**0.0004**	**−0.5555**	**−0.9340**	**−0.9856**	**−0.4443**	**−0.0638**	**−0.0141**
6	**0.0479**	**0.2017**	**0.0054**	**0.9521**	**0.7983**	**0.9946**	**−0.2368**	**−0.0082**	**−0.3860**	**0.2521**	**−6.3327**	**0.4855**	**0.0004**	**0.0002**	**0.0002**	**−0.9521**	**−0.7983**	**−0.9944**	**−0.0478**	**−0.2014**	**−0.0054**
7	**0.1954**	**0.0635**	**0.1654**	**0.8046**	**0.9365**	**0.8346**	**−0.0403**	**−0.3380**	**−0.5309**	**−0.5336**	**0.7666**	**−14.6083**	**0.0006**	**0.0001**	**0.0001**	**−0.8045**	**−0.9363**	**−0.8343**	**−0.1953**	**−0.0634**	**−0.1653**
8	**0.2566**	**0.0043**	**0.0491**	**0.7434**	**0.9957**	**0.9509**	**−1.7193**	**−0.0516**	**−0.5548**	**0.2223**	**0.9771**	**−3.7945**	**0.0002**	**0.0002**	**0.0001**	**−0.7432**	**−0.9953**	**−0.9507**	**−0.2565**	**−0.0043**	**−0.0490**
9	**0.0407**	**0.3849**	**0.0013**	**0.9593**	**0.6151**	**0.9987**	**−0.0958**	**−0.1637**	**−0.5058**	**0.2371**	**−0.3731**	**0.8738**	**0.0003**	**0.0001**	**0.0001**	**−0.9592**	**−0.6148**	**−0.9981**	**−0.0407**	**−0.3845**	**−0.0013**
10	**0.9526**	**0.0439**	**0.0990**	**0.0474**	**0.9561**	**0.9010**	**−0.0614**	**−0.3197**	**−1.0868**	**−3.6994**	**0.9242**	**−8.7023**	**0.0005**	**0.0001**	**0.0002**	**−0.0474**	**−0.9552**	**−0.9009**	**−0.9522**	**−0.0439**	**−0.0988**
USA	**0.4519**	**0.3754**	**0.0522**	**0.5481**	**0.6246**	**0.9478**	**−1.6368**	**−0.0000**	**−1.0838**	**−1.6978**	**−0.6591**	**−3.5747**	**0.0005**	**0.0002**	**0.0002**	**−0.5481**	**−0.6242**	**−0.9475**	**−0.4517**	**−0.3748**	**−0.0521**

5. Disclosures and declarations

No funding was received for conducting this study. The research does not include any human or animal participants.

Data availability

The data used in this study are available online as described in Section3.

Declaration of competing interest

There is no conflict of interest concerning the work done here. All authors certify that they have no affiliations with or involvement in any organization or entity with any financial interest or non-financial interest in the subject matter or materials discussed in this manuscript.

References

Annual Population Estimates. Estimated components of resident population change, and rates of the components of resident population change for the United States, states, District of Columbia, and Puerto Rico. https://www.census.gov/data/tables/time-series/demo/popest/2020s-state-total.html. United States Census Bureau.

Araf, Y., Akter, F., Tang, Y-d, Fatemi, R., Parvez, S. A., Zheng, C., & Hossain, G. (2022). Omicron variant of SARS-CoV-2: Genomics, transmissibility, and responses to current COVID-19 vaccines. *Journal of Medical Virology, 94*, 1825–1832. https://doi.org/10.1002/jmv.27588

Arruda, E. F., Das, S. S., Dias, C. M., & Pastore, D. H. (2021). Modelling and optimal control of multi strain epidemics, with application to COVID-19. *PLoS One, 16*(9), Article e0257512. https://doi.org/10.1371/journal.pone.0257512

Bentaleb, D., Harroudi, S., Amine, S., & Allali, K. (2020). Analysis and optimal control of a multistrain SEIR epidemic model with saturated incidence rate and treatment. *Differential Equations and Dynamical Systems*. https://doi.org/10.1007/s12591-020-00544-6

Centers for Disease Control and Prevention (CDC). SARS-CoV-2 monitoring variant proportions. https://data.cdc.gov/Laboratory-Surveillance/SARS-CoV-2-Variant-Proportions/jr58-6ysp. United States COVID-19 Variant Proportions CDC 2022.

Centers for Disease Control and Prevention (CDC). (2022a). *Data. United states COVID-19 cases and deaths by state over time*. CDC Centers for Disease Control and Prevention (cdc). https://data.cdc.gov/Case-Surveillance/United-States-COVID-19-Cases-and-Deaths-by-State-o/9mfq-cb36.

N. G. Davies, S. Abbott , R. C. Barnard , C. I. Jarvis , A. J. Kucharski , J. D. Munday , C. A. B. Pearson , T. W. Russell , D. C. Tully , A. D. Washburne , T. Wenseleers , A. Gimma , W. Waites , K. L. M. Wong , K. van Zandvoort , J. D Silverman, CMMID COVID-19 Working Group, COVID-19 Genomics UK (COG-UK) Consortium, K. Diaz-Ordaz Davies, N.G., et al. (2021). Estimated transmissibility and impact of SARS-CoV-2 lineage B.1.1.7 in England. Science, 372, eabg3055.

Dhawan, M., Saied, A. A., Mitra, S., Alhumaydhi, F. A., Emran, T. B., & Wilairatana, P. (2022). Omicron variant (B.1.1.529) and its sublineages: What do we know so far amid the emergence of recombinant variants of SARS-CoV-2? *Biomedicine & Pharmacotherapy, 154*, Article 113522.

Driessche, P. V., & Watmough, J. (2002). Reproduction numbers and sub-threshold endemic equilibria for compartmental models of disease transmission. *Mathematical Biosciences, 180*, 29–48. B.1.1.529 variant has the second highest transmission rate.

Fudolig, M., & Howard, R. (2017). The local stability of a modified multi-strain SIR model for emerging viral strains. *PLoS One, 15*(12), Article e0243408. https://doi.org/10.1371/journal

Hachmann, N., Miller, J., Collier, A. Y., Barouch, D., & Neutralization. (2022). Escape by SARS-CoV-2 omicron subvariant BA.4.6. *New England Journal of Medicine, 387*, 1904–1906. https://doi.org/10.1056/NEJMc2212117

Hattaf, K., Mohsen, A. A., Harraq, J., & Achtaich, N. (2021). Modeling the dynamics of COVID-19 with carrier effect and environmental contamination. *International Journal of Modeling, Simulation, and Scientific Computing, 12*(3), Article 2150048.

He, D., Zhao, S., Lin, Q., Zhuang, Z., Cao, P., Wang, M. H., & Yang, L. (2020). The relative transmissibility of asymptomatic COVID-19 infections among close contacts. *International Journal of Infectious Diseases, 94*, 145–147.

Khyar, O., & Allali, K. (2020). Global dynamics of a multi-strain SEIR epidemic model with general incidence rates: Application to COVID-19 pandemic. *Nonlinear Dynamics, 102*, 489–509. https://doi.org/10.1007/s11071-020-05929-4

Kislaya, I., Casaca, P., Borges, V., Sousa, C., Ferreira, B. I., Fonte, A., & Peralta-Santos, A. (2023). Comparative effectiveness of COVID-19 vaccines in preventing infections and disease progression from SARS-CoV-2 omicron BA.5 and BA.2, Portugal. *Emerging Infectious Diseases, 29*(3), 569–575. https://doi.org/10.3201/eid2903.221367

Lagarias, J. C., Reeds, J. A., Wright, M. H., & Wright, P. E. (1998). Convergence properties of the Nelder-Mead simplex method in low dimensions. *SIAM Journal on Optimization, 9*(1), 112–147.

Liu, Y., & Rocklòv, J. (2022). The effective reproductive number of the Omicron variant of SARS-CoV-2 is several times relative to Delta. *Journal of Travel Medicine*, 1–4. https://doi.org/10.1093/jtm/taac037

Liu, Y., & Rocklov, J. (2022). The effective reproductive number of the Omicron variant of SARS-CoV-2 is several times relative to Delta. *Journal of Travel Medicine, 29*(3), taac037.

Liu, Y., Zhao, S., Ryu, S., Ran, J., Fan, J., & He, D. (2022). Estimating the incubation period of SARS-CoV-2 Omicron BA.1 variant in comparison with that during the Delta variant dominance in South Korea. *One Health, 15*, Article 100425.

Massard, M., Eftimie, R., Perasso, A., & Saussereau, B. (2022). A multi-strain epidemic model for COVID-19 with infected and asymptomatic cases: Application to French data. *Journal of Theoretical Biology, 545*, Article 111117.

Meehan, M. T., Cocks, D. G., Trauer, J. M., & McBrydea, E. S. (2018). Coupled, multi-strain epidemic models of mutating pathogens. *Mathematical Biosciences, 296*, 82–92.

Nelder, J. A., & Mead, R. (1965). A simplex method for function minimization. *The Computer Journal, 7*, 308–313.

Nisar, K. S., Ahmad, S., Ullah, A., Shah, K., Alrabaiah, H., & Arfan, M. (2021). Mathematical analysis of SIRD model of COVID-19 with Caputo fractional derivative based on real data. *Results in Physics, 21*, Article 103772.

Nishiura, H., Ito, K., Anzai, A., Kobayashi, T., Piantham, C., & Rodríguez-Morales, A. J. (2022). Relative reproduction number of SARS-CoV-2 omicron (B.1.1.529) compared with Delta variant in South Africa. *Journal of Clinical Medicine, 11*, 30. https://doi.org/10.3390/jcm11010030

OASH Regional Offices. The U.S. Department of health and human Services. https://www.hhs.gov/ash/about-ash/regional-offices/index.html.

Ogata, T., & Tanaka, H. (2023). SARS-CoV-2 incubation period during the omicron BA.5- dominant period in Japan. *Emerging Infectious Diseases, 29*(3). www.cdc.gov/eid.

Otunuga, O. M. (2021). Estimation of epidemiological parameters for COVID-19 cases using a stochastic SEIRS epidemic model with vital dynamics. *Results in Physics, 28*, Article 104664.

Otunuga, O. M. (2022). Analysis of multi-strain infection of vaccinated and recovered population through epidemic model: Application to COVID-19. *PLoS One*. https://doi.org/10.1371/journal.pone.0271446

PAHO/WHO. (2022a). Epidemiological alert: Increase of COVID-19 cases and hospitalizations. Pan American health organization (PAHO); world health organization (WHO). Available at: https://www.paho.org/en/documents/epidemiological-alert-increase-covid-19-cases-and-hospitalizations.
PAHO/WHO. (2022b). *Emergence of sublineages and recombination events: Genetic evolution of SARS-CoV-2*. Available at: Pan American Health Organization (PAHO); World Health Organization (WHO) https://www.paho.org/en/documents/emergence-sublineages-and-recombination-events-genetic-evolution-sars-cov-2-13-april-2022.
Rahimi, J. F., & Abadi, A. T. B. (2022). The Omicron subvariant BA.2: Birth of a new challenge during the COVID-19 pandemic. *International Journal of Surgery, 99*.
Rui, J., Zheng, J.-X., Chen, J., Wei, H., Yu, S., Zhao, Z., Wang, X.-Y., Chen, M.-X., Xia, S., Zhou, Y., Chen, T., & Zhou, X.-N. (2022). Optimal control strategies of SARS-CoV-2 Omicron supported by invasive and dynamic models. *Infectious Diseases of Poverty, 11*, 115. https://doi.org/10.1186/s40249-022-01039-y
Saltelli, A., Tarantola, S., & Campolongo, F. (2000). Sensitivity analysis as an ingredient of modeling. *Statistical Science, 15*(4), 377–395.
Tartof, S. Y., Slezak, J. M., Puzniak, L., Hong, V., Frankland, T. B., Ackerson, B. K., Takhar, H., Ogun, O. A., Simmons, S., Zamparo, J. M., Jodar, L., & M McLaughlin, J. (2022). BNT162b2 vaccine effectiveness against SARS-CoV-2 omicron BA.4 and BA.5. *CORRESPONDENCE— VOLUME, 22*(12), P1663–P1665.
Tegally, H., Moir, M., Everatt, J., Giovanetti, M., Scheepers, C., Wilkinson, E., Subramoney, K., Makatini, Z., Moyo, S., Amoako, D. G., Baxter, C., Althaus, C. L., Anyaneji, U. J., Kekana, D., Viana, R., Giandhari, J., Lessells, R. J., Maponga, T., Maruapula, D., Tegally, H., Moir, M., andEveratt, J., et al. (2022). Emergence of SARS-CoV-2 omicron lineages BA.4 and BA.5 in South Africa. *Nature Medicine, 28*, 1785–1790.
Tiecco, G., Storti, S., Arsuffi, S., Antoni, M. D., Focá, E., Castelli, F., Quiros-Roldan, E., & Omicron, B. A. (2022). 2 lineage, the "Stealth" variant: Is it truly a silent epidemic? A literature review. *International Journal of Molecular Sciences, 23*, 7315. https://doi.org/10.3390/ijms23137315
Ueda, M., Kobayashi, T., & Nishiura, H. (2022). Basic reproduction number of the COVID-19 Delta variant: Estimation from multiple transmission datasets. *Mathematical Biosciences and Engineering, 19*(12), 13137–13151. https://doi.org/10.3934/mbe.2022614
Wang, S., Zhang, F., Wang, Z., Du, Z., & Gao, C. (2022). Reproduction numbers of SARS-CoV-2 Omicron subvariants. *Journal of Travel Medicine*, 1–3. https://doi.org/10.1093/jtm/taac108
Xin, H., Wang, Z., Feng, S., J Cowling, B., Kong, Q., & Wu, P. (2023). Transmission dynamics of SARS-CoV-2 omicron variant infections in hangzhou, zhejiang, China, january-february 2022. *International Journal of Infectious Diseases, 126*, 132–135.

Further reading

Burki, T. K. (2022). Omicron variant and booster COVID-19 vaccines. *Lancet Respiratory Medicine, 10*(2), E17–E.
Kulpa, W. (1997). The poincaré-miranda theorem. *The American Mathematical Monthly, 104*(6), 545–550.
Kumar, S., Karuppanan, K., & Subramaniam, G. (2022). Omicron (BA.1) and sub-variants (BA.1.1, BA.2, and BA.3) of SARS-CoV-2 spike infectivity and pathogenicity: A comparative sequence and structural-based computational assessment. *Medical Virology, 94*(10).
Martcheva, M. (2015). *An introduction to mathematical epidemiology, 61*. New York Heidelberg Dordrecht London: Springer.
Mastrorosa, I., Cozzi-Lepri, A., Colavita, F., Lalle, E., Mazzotta, V., Cimaglia, C., … Antinori, A. (2022). SARS-CoV-2 nasopharyngeal viral load in individuals infected with BA.2, compared to alpha, gamma, Delta and BA.1 variants: A single-center comparative analysis. *Journal of Clinical Virology*, 157.
The United States Center for Disease and Control. Information on OMICRON variant. https://cdc.gov/coronavirus/2019-ncov/variants/omicron-variant.
The United States Center for Disease and Control. Information on DELTA variant. https://cdc.gov/coronavirus/2019-ncov/variants/delta-variant.html.
US government SARS-COV-2 Interagency Group (SIG).. https://cdc.gov/coronavirus/2019-ncov/variants/variant-info.html.
Wang, Q., Li, Z., Ho, J., Guo, Y., Yeh, A. Y., Mohri, H., … Ho, D. (2022b). Resistance of SARS-CoV-2 omicron subvariant BA.4.6 to antibody neutralisation. *CORRESPONDENCE, 22*(12), P1666–P1668.
WHO. Weekly epidemiological update on COVID-19. 8 June 2022. Available online: https://www.who.int/publications/m/item/weekly-epidemiological-update-on-covid-19-8-june-2022 (accessed on 9 June 2022).
Yang, Z.-R., Jiang, Y.-W., Li, F.-X., Liu, D., Lin, T.-F., Zhao, Z.-Y., … Tang, J.-L. (2023). Efficacy of SARS-CoV-2 vaccines and the dose-response relationship with three major antibodies: A systematic review and meta-analysis of randomised controlled trials. *Lancet Microbe, 4*, e236–e246.